

MASTER'S THESIS

L

Lucerne Train Station-Trial Shaft, a Case Study using HS-ss Model with Plaxis 3D

Carlos Rojas
2016

Master of Science (120 credits)
Civil Engineering

Luleå University of Technology
Department of Civil, Environmental and Natural Resources Engineering



Acknowledgements

I like to thank three groups of people that have made this dissertation possible.

The first group is composed by the thesis supervisor Prof. Hans Mattsson, who has act as a reference for the Finite element analysis and geotechnics. Equally important has been Prof. Jan Laue, who has provided me with the opportunity to work with this project and for his comments regarding the interpretation of results.

The second group is made up of my colleagues at LTU. Special thanks to Jonas Majala, that at the distance was always there to assist with the running of the last models as required in the last part of the thesis.

The third group is my family. All my gratitude and love to my wife, Dr. Juana Isabela Ordonez, who at all times has provided me with the necessary support, showing a great deal of patience and interest in my development.

Many thanks to my sister Yili Maria, that has always believed in me and has provided me with the inspiration to look always for new horizons.

Table of Contents

Abstrakt.....	5
Abstracts.....	6
1. Preliminaries.....	7
1.1. Generalities about the Lucerne extension project.....	7
1.2. Information and materials	8
1.3. Software	8
1.4. Thesis objectives	8
Task to perform.....	9
1.5. Briefing on report sections.....	9
2. Geology	10
2.1. Switzerland geology	10
2.1.2. Geological profile of the Plateau.....	10
2.1.3 Geotechnical properties of Lucerne soils.....	11
2.1.4. Determination of soil parameters.....	11
3. Underground water.....	13
4. Geotechnical profile	15
5. Trial shaft construction design aspects.....	18
5.1. Design failure.....	19
6. Theory review.....	21
6.2 Diaphragm walls design - analytical solutions	21
Empirical methods	22
Semi-empirical methods	22
Analytical methods.....	23
Limit equilibrium method	24
D-wall supported with multiple struts	25
Elastic methods	27
7. The Finite element method.....	27
7.1. Development of FEM.....	27
7.2. 3D finite element analysis.....	28
7.2.1. Finite element analysis using 3D modelling.....	29
Displacement space	29
Strain field	29

Stress field	30
Strain stress correlation	30
8. Constitutive model used in numerical analysis of soils.....	30
8.1. Mohr Coulomb model	31
8.2. Hardening Soil model	32
8.3 Hardening Soil with small strains.	34
8.4. Linear elastic model	35
Preliminary remarks about Plaxis numerical modelling.....	35
9. Modelling work flow	36
9.1. Model parameters.....	37
Mesh parameters	40
Calculation steps	41
Results	42
1. M-C model variations results	42
2. HS-ss model variations results	42
3. HS-ss models using struts HEB 300 and HEB 450 struts.....	43
4. Verification of 3D model with struts HEB 300 using PLAXIS 2D AE model.....	44
9.2. Model parameters.....	44
10. Layer B collapse.....	46
11. Sensitivity analysis.....	48
12. Discussion.....	49
13. Conclusions and recommendations	51
14. Suggestions for future studies.	52
Appendix A. Geological profile for the area where the future underground railway is planned	53
Appendix B . Floor plan of the trial shaft where the boreholes are used for the geotechnical profile and for the material properties (M9) are shown. B&H AG, 2012.....	54
Appendix C. Shaft with the allocation of the bore holes used for the 3D and 2D modelling.	55
Appendix D. Odometer test results bore hole M9 and corresponding values for HS-ss.	56
Appendix E. Cambridge test results test results from where Go and $\gamma_0, 7$ bore hole M4.....	57
Appendix F. Pore pressures as per bore hole user define pressures.	58
Appendix G. Relation of layers that are in contact with D-walls.....	59
Appendix H. Bending moment 3D view and lateral displacement 300 HEB	60
Appendix I. D-wall ending moments HS-ss model HEB 300 and 450 100x200	61

Appendix J. 3 D model. D-wall bending moments HS-ss HEB 300	62
Appendix K. Struts forces by construction steps HEB 300	63
Literature.....	64

Abstrakt

Den nya Trans alpina tunneln, Gottard tunnel som ansluter södra och norra Schweizuppskattas få en ökning på 45% av passagerarna av de federala myndigheterna. Detta kommer att kräva en uppdatering av de befintliga stationerna och utbyggandet av nya länkar som kan ta upp den ökade efterfrågan på nya infrastrukturen. För den nämnda uppdateringen av den nationella järnvägens rutnät, är en uppdatering av centralstationen Lucerne att betrakta som ett måste. Lucerne järnvägsstation stiger som en knutpunkt för transport i Schweiz och ger inte bara anslutningar på lokal och regional nivå, men även på en internationell nivå.

Utbyggnationen av Lucerne tågstation innebär en byggnation av en underjordisk nivå av spår där plattformar för avgångar och ankomster kommer att tilldelas.

På grund av sitt läge så är förhållandena i jorden av en komplex mjuk mark jordbädd och förekomsten av två distinkta freatiskt nivåer existerar.

Under grunddesign fasen bestämde den schweiziska federala järnvägsmyndigheten (SBB) att driftsätta exekvering av försöksaxeln för att bedöma konstruktionen av kvarhållningssystem som använder sig av membran väggar.

Försöksaxeln var utrustad med dragmätare för att mäta tryck- och eventuella utböjningar av väggen och det bärstöd som användes. Resultaten av plats observationer bevisar att utformningen av stödsystemet inte var tillräcklig, som i stället kräver extra stål stöttor för att förhindra en eventuell kollaps av axeln.

Föreliggande examensarbete är den andra studien som har genomförts för att analysera inverkan av befintliga markbädden med fokus på den mjuka sandskiktet, och det strukturella systemet.

Studien sker efter den analys och de förslag som gjordes i den första studien där användningen av en ändliga elementkoden för geotekniska arbeten PLAXIS 3D rekommenderats, med tanke på variabiliteten av skikten vid den punkt där testaxeln har konstruerats.

Beräkningarna görs först genom att utföra en Mohr Coulomb modell följt av en härdningsjord med små stammar (HS-ss) modellvarianter.

Slutresultatet valideras med hjälp av 3D-modell och genom att jämföra resultaten med tidigare 2D analyser.

Kollaps analys för en av de känsliga skikt som finns i projektet, skikt B, presenteras därefter för att ytterligare förstå de möjliga orsakerna till en kollaps av detta skikt och dess möjliga bidrag vid fel på instabiliteten hos D-väggarna. Känslighetsanalysen görs på vid den sista delen av studien för att definiera modellens beteende under byggnation och efter byggnation, där laster för båda fallen beaktas.

Abstract

The new Trans alpine tunnel, Gottard tunnel that connects the south and north of Switzerland and the forecast of the federal authorities estimating an increment of 45% of passengers demands the update of the existing stations and the construction of new links that can take up the future demand of transportation. Within the mentioned update of the national rail grid the Lucerne train station update is considered a must, as Lucerne rises as a transportation hub within Switzerland providing not only connections at the local and regional level but also at the international one.

The enlargement of the Lucerne train station includes the construction of an underground level where departures and arrivals platforms will be allocated. Due to its location the soil conditions are given by complex soft soil bedding and the existence of two distinctive phreatic levels.

During the base design face the Swiss federal railways authority (SBB) has commission the execution of the trial shaft in order to assess the construction of retaining system using a Diaphragm walls.

The trial shaft was equipped with tension gauges to measure the pressure and possible deflections of the wall and support used. The results of the on-site observations proof that the design of the support system was not sufficient, requiring extra steel struts to prevent a possible collapse of the shaft.

The present master thesis is the second study that is done in order to analyse the influence of the soil bedding specially the sand layers, and the structural system. The analysis is done following the analysis and suggestions made in the first study where the use of a finite element code for geotechnical works, PLAXIS 3D considering the variability of the layers at the point where the trial shaft has been constructed.

The calculations are done first by performing a Mohr coulomb model followed by a Hardening soil with small strains (HS-ss) model variations. The final result is validated by the use of PLAXIS 2D using the same parameters as for the 3D model using the variation of 100x200.

The collapse analysis for one of the sensible layers found in the project, layer B is then presented to further understand the possible causes for the collapse of this layer and its possible contribution in case of the adjacent soils and shaft failure.

The sensitivity analysis is done in the last part, to assess the behaviour of the trial shaft, during construction.

1. Preliminaries

1.1. Generalities about the Lucerne extension project

The federal transportation authorities of Switzerland estimate a 45% increment of commuters by the year 2030. This prospect and the continual increment of travelers using the train not only on a local or regional basis, but in the international ones, have raised the demand for the update of the existing train stations. Lucerne central train station will play an important role in the new dynamics of the rapid transit rail network in Switzerland.

Lucerne central station is the 5th largest station in Switzerland where more than 60.000 trips are done per day using the station. No major update of the station has been done in the last 100 years and now considering the actual population growth and the future demands the construction of new corridors such as the Gotthard tunnel that will bring more passengers to Lucerne, the administration has plan to undertake the necessary works to update the station and undertake the changes at the entrance of the station as the bottle neck rail track is not any longer a solution considering the connection with Zurich as well as the existing subway connection with Ebriko. The update considers an underground level for the new tracks in the station that will be able to attend some 400 train arrivals per day, shortening the transit tie in the connection to Zurich in 30 minutes.

The project comprises three main parts, the underground metro station with some 450 meter in length,

3.5 Km of twin tunnels and the direct connection with Ebriko, marked with a gray line. In Figure.1

For the purpose of the present work the analysis is only perform for the part of the underground station at Lucerne Central station.

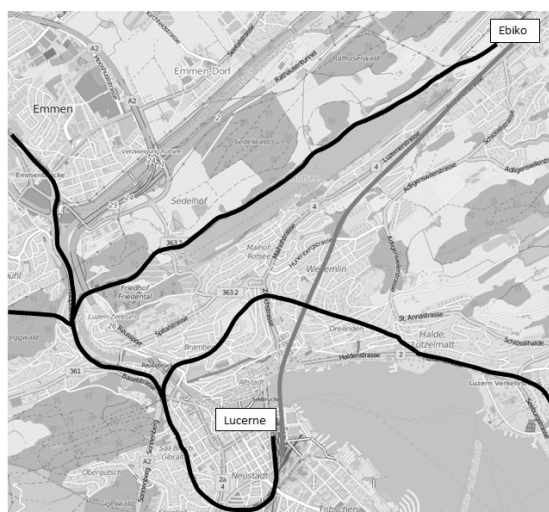


Figure.1. Market in black existing track. In gray, the proposed direct link Lucerne - Ebriko

1.2. Information and materials

The present work is part of a set of proposed studies, with the aim to understand the mechanical properties, and therefore soil-structure interaction, at the area where the future underground level tracks of the Lucerne Central station will be constructed. The materials and values used in this study have been taken from the first study by Maria Antri , 2015. and has therefore used the same documentation regarding the geohydrology and geotechnical properties of the existing soil layers, that include test results used in the first study from where values for the Hardening Soil with small strains parameters have been derived.

The following is a relation of the documentation that was used in the first study and from where most of the values and definitions on geotechnical properties for the numerical model were extracted for the present work.

1. Geological study Keller + Lorenz AG :
The Underground station Lucerne, bases for preliminary project that includes Geology, Hydrology and Geotechnics.
2. Geotechnical office Geoprofile GmbH
Preliminary underground station, Lucerne Electrical CPT results
Preliminary underground station, Lucerne, determination of soil liquefaction potential by electrical CPT
3. Basler & Hofmann AG
General plan, situation 1: 5000, Plan No. 4655.1.001, date 14.02.11
Underground station, cross section 1: 200, No. 4655.1.012 date 14.02.11
Installation plan before trial shaft construction, plan no. 6003.21.-05B date 07.05.12
Schiitzawand – Overview diagram attempt tray 1 : 100, Plan No. 6003 -06B, date 11.05.12

1.3. Software

The numerical code used PLACIS 2D AE and 3D AE, 2015.

1.4. Thesis objectives

In a previous study done by M.Antri, 2015, the analysis of the trial shaft was done using PLAXIS 2D classic, and the focus was on a series of variations in the soil layers that were mainly analyzed using a Mohr Coulomb model. Following the suggestions made in the first study by Antri, 2015 the present thesis focus on the 3D modelling of the trial shaft in Lucerne central station, using Hardening soil with small strains, to further investigate the behavior of the existing soils and the soil structure interaction with the trial shaft in particular for layer B, a soft material layer, where an intermediate aquifer is found.

Task to perform

To reach the mention objective, the related theory to excavation in soft soils, stability of excavations supported using multiple struts; the construction of D walls and the related ground water protection that governs the design on the previous study is reviewed as well as finite element method and used models, followed by:

- The review and study of Plaxis 3D AE tutorials to gain sufficient understanding of the program in order to perform the modelling of the trial shaft using Mohr-Coulomb and Hardening Soil with small strains.
- The analysis and interpretation of the results where both Mohr-Coulomb and HS-ss are compared.
- The collapse model of the soft silty sand layer, and the sensitivity analysis where the trial shaft is tested using different loads as could take place during construction and after construction.

1.5. Briefing on report sections

The present report is made out of 13 sections.

Section 2, presents the geological environment where the project takes place providing sufficient information to continue with the geotechnical profiles that are used in this work that included the hydrological conditions found under the Lucerne train station where the underground station is projected. In this section all the assumptions that are part of the materials are listed and explained.

Section 3 and 4, presents the location of the trial shaft in the Lucerne station is introduced as well as the constructive method and measured equipment that was installed followed by an outline of the discussion part of the first analysis.

Section 5, present the construction aspects of the trial shaft as constructed.

Sections 6, 7 and 8 review the theory of D-wall analytical solutions, the FEM and its use within geotechnics, covering the models used as well as the model processing, material properties, meshing, underground water levels, calculation steps and variations on models size. In this section the results of the numerical analysis are presented.

Section 9, covers the calculation of the models. In this section is the analysis and interpretation part of the report where the values from the Mohr-Coulomb and the HS-ss are compared.

Sections 10 and 11, present the collapse of layer B and the sensitivity analysis of the model.

Sections 12 and 13, present the discussion, conclusions and recommendations accordingly.

2. Geology

2.1. Switzerland geology

The geology of Switzerland can be described as the collection of three distinctive geographical areas that are determined by its geology; The Jura, the plateau, and the Alps region. See figure.2.

- The Jura is a mountain chain formation dating back to the Jurassic period mainly composed of limestone and a large quantity of fossils from where it inherited its name.
- The Plateau is located between the two mountain ranges, Jura and Alps, being at the lowest point among the three zones is where most of the lakes in Switzerland are located. It is characterized by the presence of sediment material from previous sea bodies during the Jurassic period and of sediments that were transported due to later weathering and erosion process from the Alps and Jura mountain ranges.
Is in this area where the project is located and therefore where the focus on the geology will be placed. TP Labhart, (1987)
- The Alps are located in the southern part of the country and are part of a mountain range system that starts in the Mediterranean expanding along central Europe. The mountains formations are composed by sedimentary rocks and were formed by the collision of the Euro-Asian plate and the African plate. TP Labhart, (1987).

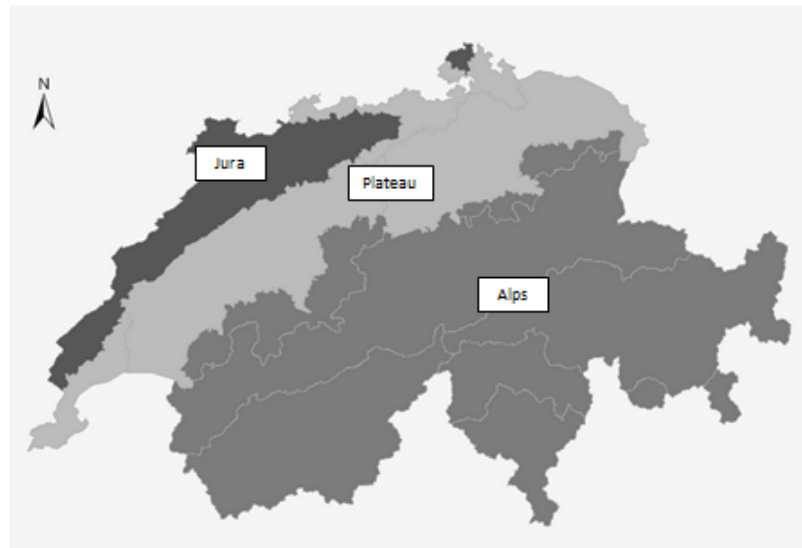


Figure.2. Geographical zones of Switzerland

2.1.2. Geological profile of the Plateau

The Plateau is composed of a crystalline basement that forms a geosyncline that is likely to be filled with sandstone with lots of rock fragments and clay materials located some - 2500 - 3000 meters. Above this layer it is found an unfolded stratum of Mesozoic limestones, shales and marls that can be part of the Helvetic thrust sheet ranging in thickness of 2500 m to 800 meters. The next layer found is the combined sandstones, shales and conglomerate

shallow marine deposits. The last layer is made out of glacial sediments and gravel that was transported and deposited by the glaciers during the ice ages.

All this layers are considered to be as disturbed material due to its passed history where at different geological periods the shallow sea entered and receded forming the conglomerate fan found in Napf region, where Lucerne is located, some 22 – 16 million years ago first and after when it receded continuing with the forming of the Napf sediment fan . TP Labhart, (1987).

2.1.3 Geotechnical properties of Lucerne soils

As mentioned before, the trial shaft is constructed in the railway station to find the mechanical properties of the different soil layers and the responds of the proposed structural system.

The geotechnical properties of the existing soil layers under the Lucerne railway station are formed of a various glacial and postglacial soft alluvial deposits, Clay, silt, fine sand and gravel beddings that came about as a result of different sedimentation processes that where mentioned before. The sand deposits after the clay layer defined the existing artesian aquifer, presenting a high permeability therefore, been quiet sensible ground. If a groundwater relief where to take place subsidence is likely to occur. The same is true for the intermediate aquifer found in the soft layer B. Above this layer is layers A1 and A2 is found the free aquifer. In this study the intermediate and the free aquifer are treated as been one. The following is a description of the soil units found at the site where the trial shaft is excavated.

Table.1. Layer soil material description Lucerne train station

Soil description as per layer found		
Soil layer ID	Type of soil	Description
A1	Artificial filling	Very soft sand silt clay layers where with organic sediments and where the first aquifer is found.
A2	Clay silt and silty sand	Very soft sand rich layer with finer grain sizes
B	Silty sand	Tight sand alluvial depot with small proportion of fine grains where layers of sand and thin silt layers are superimposed.
C	Silty Clay	Soft and loose clay layer that serves as a separation for the second aquifer found.
D1	Sand	Mid compacted / medium dense alluvial deposit with turbities.
D2	Sand	Tightly compacted deposit with some Lents of moraine

2.1.4. Determination of soil parameters

The determination of the soil parameters was done considering the soil condition that where determined by the use of electrical CPT. They are two sets of measurements, one done in the area where the trial shaft is located and other following the alignment of the future metro project connection. The interpretation of the results is based on theoretically based correlations where permeability can be estimated by the penetration cone test as it measure the development of pore water pressures with time as well as the density.(See table.1.)

It is equally important to underline that the values used are those obtained from the measurements performed for the metro line from Lucerne station and not those from the location of the trial shaft as in these measurements the soil layers are found to be more compacted been and therefore been stiffer. The soil properties where adjusted using the electrical CPTs CPTU, Keller and Lorenz, (2010). The value for the cohesion is zero due to the fact that there are no readings for the undrained shear strain.

The location of the transition zone between layers C and D explain the change in the layers levels within a few meters. (See figure.7.) This is the location of the trial shaft.

It is also important to mention that the soils potential for liquefaction were evaluated for lateral and vertical deformation following the method by Robertson and Write, (1998).

In general, deformation in all soils can be expected as all soils develop a given pore pressure during cyclic loading at small strains these pore pressures are in most cases positive. In the case of sand, the development of pore pressure is high when experiencing cyclic loading and it is possible to reach a condition of zero effective confining stress, in such conditions the initial structure of the soil is lost and the stiffness of the soil in shear is near zero, in this form large deformations occur during an earthquake. Boulanger and Idriss, (2004, 2007). The analysis for the soils at Lucerne central station were based on the historical data, CPTs, CPTU 2, 3, and 4, considering an earthquake of magnitude 6 and 6.5 in the richter scale.

Table.2. soil properties according to Keller + Lorenz (2010) results are those part of the metro connection alignment project.

Schicht	γ [kN/m ²]	ϕ' [°]	c' [kN/m ²]	k [m/s]	ME [MN/m ²]
A1: Künstliche Auffüllungen	16.5±20.0	28±35	0	$10^{-3} \pm 10^{-7}$	-
A2: Verlandungsbildungen	17.5±18.5	25±30	0	$k_v \pm 10^{-7} \pm 10^{-9}$ $k_h \pm 10^{-5} \pm 10^{-9}$	1±5
B: Distale Deltaablagerungen	18.5±19.5	30±35	0	$10^{-4} \pm 10^{-5}$	5±10
C: Späteiszeitliche Gletschersee-Ablagerungen	18.5±19.5	26±28	0	$10^{-7} \pm 10^{-9}$	5±10
C: Tonig-siltige Gletschersee-Ablagerungen	18.5±19.5	26±32	0	$k_v \pm 10^{-7} \pm 10^{-9}$ $k_h \pm 10^{-5} \pm 10^{-9}$	10±20
D2: Sandreiche Gletschersee-Ablagerungen	19.5±20.5	30±35	0	$k_v \pm 10^{-7} \pm 10^{-9}$ $k_h \pm 10^{-4} \pm 10^{-9}$	20±40
D1: Sandige, Glazialakustrische Schwemmfächer	19.5±20.0	30±35	0	$10^{-4} \pm 10^{-6}$	10±25

Table.3. Customized soil properties using the test results from CPTU No. 1 and 2 on the trial shaft area.

Schicht	γ [kN/m ²]	ϕ' [°]	c' [kN/m ²]	k [m/s]	M_E [MN/m ²]
A1: Künstliche Auffüllungen	16.5±20.0	28±35	0	$10^{-3} \pm 10^{-7}$	-
A2: Verlandungsbildungen	17.5±18.5	25±30	0	$\frac{k_v \cdot 10^{-7} \pm 10^{-9}}{k_h \cdot 10^{-5} \pm 10^{-9}}$	1±5
B: Distale Deltaablagerungen	18.5±19.5	30±35	0	$10^{-4} \pm 10^{-5}$	5±10
C: Späteiszeitliche Gletschersee-Ablagerungen	18.5±19.5	20±25	0	$10^{-7} \pm 10^{-9}$	3±5
C: Tonig-siltige Gletschersee-Ablagerungen	18.5±19.5	25±30	0	$\frac{k_v \cdot 10^{-7} \pm 10^{-9}}{k_h \cdot 10^{-5} \pm 10^{-9}}$	4±12
D2: Sandreiche Gletschersee-Ablagerungen	19.5±20.5	25±35	0	$\frac{k_v \cdot 10^{-7} \pm 10^{-9}}{k_h \cdot 10^{-4} \pm 10^{-9}}$	10±15
D1: Sandige, glazialklastische Schwemmfächer	19.5±20.0	25±35	0	$10^{-4} \pm 10^{-6}$	8±12

3. Underground water

The underground water flow present in the vicinity of the studied area, have a major flow going from the south east side of the city towards the river Reuss, in parallel to the tracks at the train station (see figure.4b.), having a secondary flow direction, going under the train station towards the North side of the train station where the lake is located within 200 meters. Minor flows are also going directly to the lake in the same direction, going under the buildings located in the nearby areas to the train station. The first aquifer free aquifer, is found in the upper part of the geotechnical profile in the filling layer, the water level varies from 434,9 and 435,6 meters. (See figure.2.c), It is important to outline the existence of an intermediate aquifer that is located within layer B.

The next aquifer the artesian aquifer is found within the delta distal deposits. The extension of this deposit is not known but it is considered to exist 100 meters from where the measurement is taken the water level varies from 434,9 and 435,6 meters. This depth is therefore used for the development of the 3D analysis. (See figure.4.d)

The artesian aquifer is found under the layer of clay, where the pore pressure is larger than in the previous aquifers. The phreatic level is fount at 425,6 meter of altitude between the upper and lower part of the aquifer. The underground water flow goes to the lake via alluvial fans found in the border of the lake. (See figure.3.c.)

The found aquifers are separated by the clay layer C and therefore are not connected. Eller + Lorenz AG (2010) (See figure 4.b)

In a radio of 700 m from the train station the lower aquifer provided water to thermal baths and therefore the quality of the water must be maintained as mentioned by Anthi, 2015.

It is also important to mention that one of the main issues with the construction of the underground train platform is the groundwater protection rules that are in place for areas

where the underground water is marked as protected areas, where the upper groundwater that ends in the lake, is protected under category Ao. (Lucerne water commission, 2015) The average groundwater has not been marked in the water protection map but its protection should be observed under Ao. (See figure. 4.e)

It has been also found from adjacent excavation to the train station, that hydrogen sulfide has been liberated. Also important quantities of manganese and iron is dissolved in the groundwater, therefore any excavation in the area will cause a precipitation of this contaminants. Restrictions on how excavation works for all purposes, e.g. prospections boreholes, or excavation works for underground facilities must be considered.

The existing variation on the soil layers levels present a pore pressure difference (pore pressure game), where pore pressures the shaft are different. In this work both a hydrostatic condition using a general water level and located a -1m and a second set of models are done considering the artesian reservoir that is found after the layer of clay. Information about the groundwater found is taken from CPTU1 and 2 in accordance with the geotechnical survey done by Keller and Lorenz AG (2010). (See figure.3).

It is also clear that as the shaft excavation includes the use of a seal slab performed by the use of jet grouting columns 5m depth, the on-site conditions regarding the groundwater will not be affected.

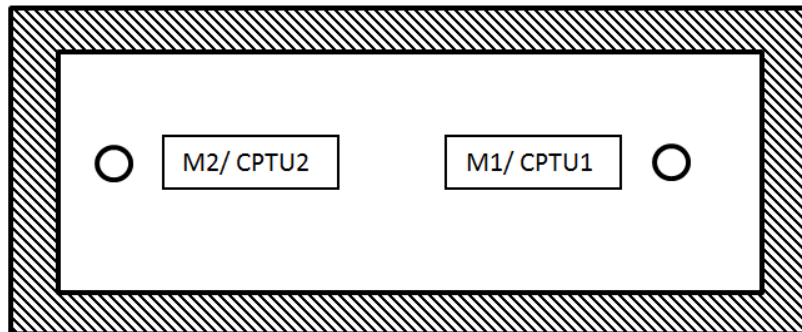


Figure.3. CPTU 1 and 2 from where ground water information is taken for further analysis in this study the shaft location is marked in the next figure using black rectangles.

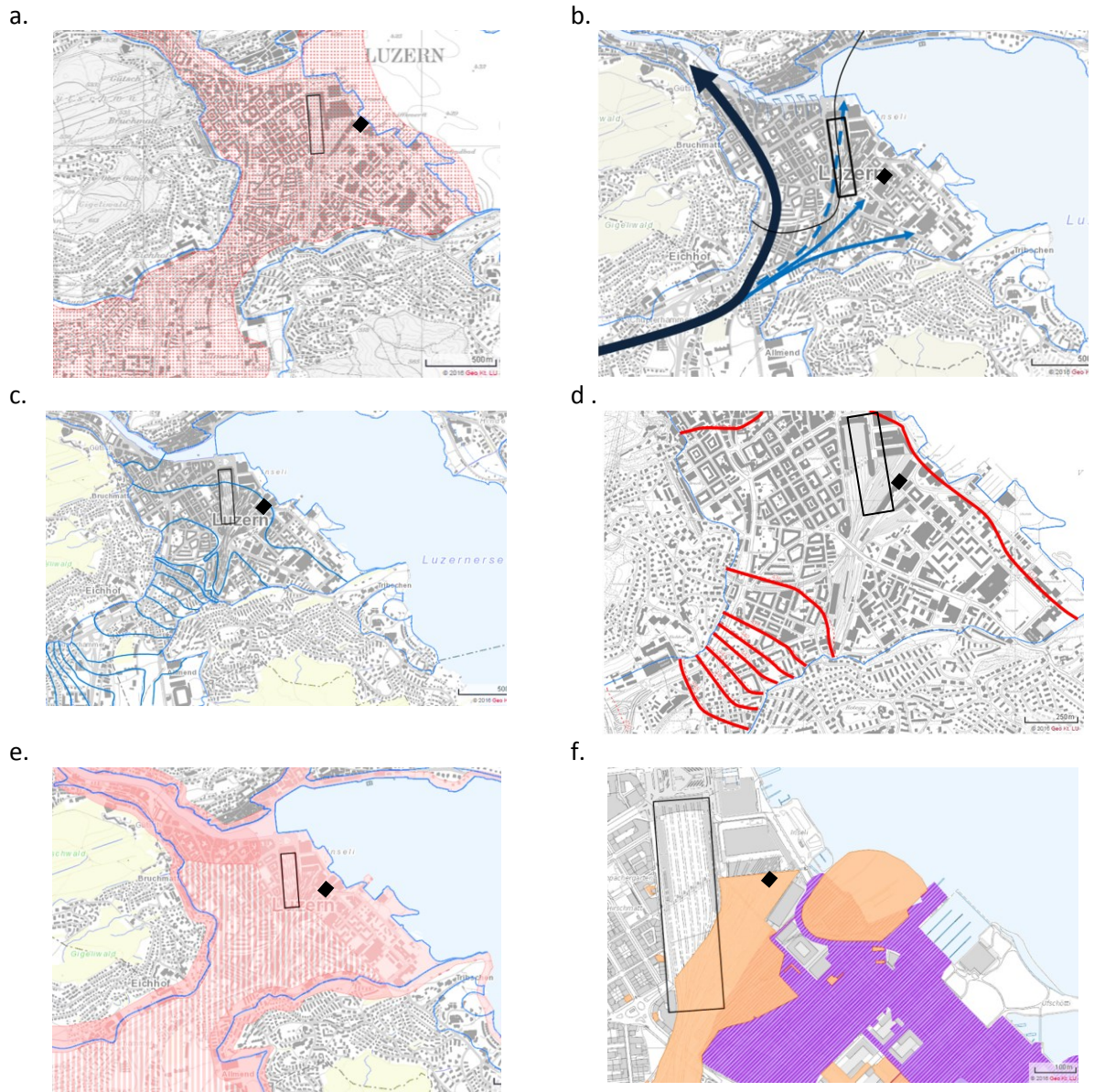


Figure 4. a Deep aquifer, b. underground water flow directions, c. Groundwater isohypsies first level, d. Groundwater pressure levels second main aquifer, e. Ground water protection area, f. contaminated area due to business activity e.g train station, and by location of deposits. In all cases the location trial Shaft is marked with a black square. Maps are prints from Metadata Canton Lucerne www.lu.ch).

4. Geotechnical profile

After reviewing the geological and hydrological aspects of the area where the underground train station is projected, a determination of geotechnical profile part of this study, is done establishing the work frame for all the analysis, discussion and conclusions in the present report. The location of all the boreholes used in the model as the Cambridge test results, are shown in figure 5 and figure 6 accordingly.

Relation of bore holes test	
Borehole ID	Drilling / testing technique used as per borehole
M6	Special drilling with grid sampling incl. installation of inclinometer and dilatometer
M2	CPTU 2 electrical testing data
M3	Special drilling with grid sampling incl. installation of inclinometer
M1	CPTU 1 electrical testing data
M4	Bored of this hole was done by using a Cambridge self-bored pressiometer

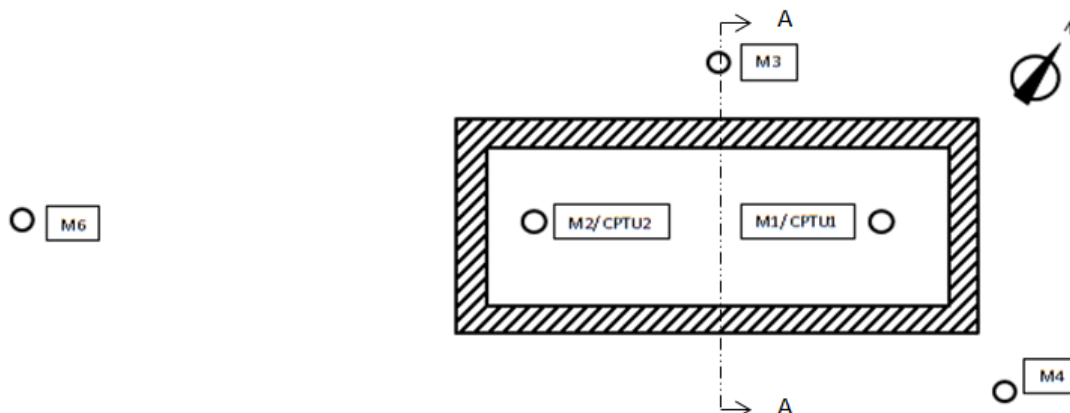


Figure.5. Floor plan with used boreholes for geotechnical profile

In order to conclude in a final geotechnical profile that will be used as a reference for 3D model analysis a summary of the material properties and comments regarding the possible behavior of found soils is done.

Table.4. Summary material geotechnical profile in accordance with B&H AG, 2012

Layer material type	Borehole material layers summary									
	Bored hole layers following the layout floor plan									
	M6		M2		M3		M1		M4	
	Top [m]	Bottom [m]	Top [m]	Bottom [m]	Top [m]	Bottom [m]	Top [m]	Bottom [m]	Top [m]	Bottom [m]
A1	0	-4	0	-2	0	-4	0	-2.5	0	-4
A2	-4	-6.5	-2	-8.5	-4	-5.5	-2.5	-11	-4	-6
B	-6.5	-9.0	-8.5	-12	-5.5	-12	-11	-17.5	-6	-9,5
C	-9.5	-27	-12	-30	-12	-13	-17.5	-29	-9,5	-18
D1	-27	-37	-30	-40	-13	-20	-29	-39	-18	-30
D2	-37	-100	-40	-100	-20	-100	-39	-100	-30	-100

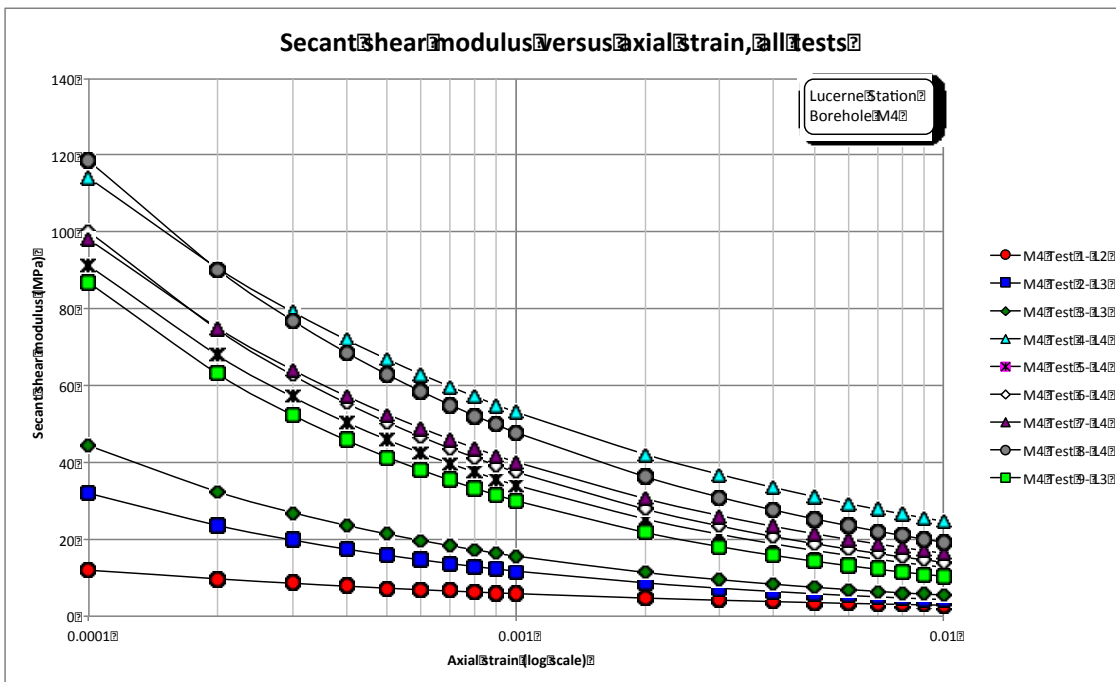


Figure 6. Self-bored Cambridge pressiometer test InsiTu Ltd, 2012

Table 6. in accordance with B&H AG, 2012 and Keller and Lorenz AG (2010)

Soil description as per layer found			
Soil layer ID	Type of soil	Description	Comments
A1	Artificial filling	Very soft sand silt clay layers where with organic sediments and where the first aquifer is found.	Very fragile material with no cohesion with presence of gravel and sand material as expected from the glacial lake deposits.
A2	Clay silt and silty sand	Very soft sand rich layer with finer grain sizes	Very fragile material with some cohesion but easy to collapse
B	Silty sand	Soft sand alluvial depot with small proportion of fine grains where layers of sand and thin silt layers are superimposed.	Layer with high permeable with an important change in thickness.
C	Silty Clay	Soft and loose clay layer that serves as a separation for the second aquifer found.	The changes in level of this layer follow the changes in layer D1, presenting some important changes within a few meters
D1	Sand	Mid compacted / medium dense alluvial deposit with turbities.	D1 and D2 layer has some 30 to 35 % of clay and is where the artesian reservoir is found.
D2	Sand	Tightly compacted deposit with some Lents of moraine	

Note:

There are more boreholes that were not included as a part of the geotechnical profile in this study, e.g. M7, M8, M9. None the less, information about the soil properties of borehole M9, was used for further investigations at the laboratory of ETH Zurich (Report no. 4790, 2012) and therefore the test results of M9, will be used at a later stage in this study.

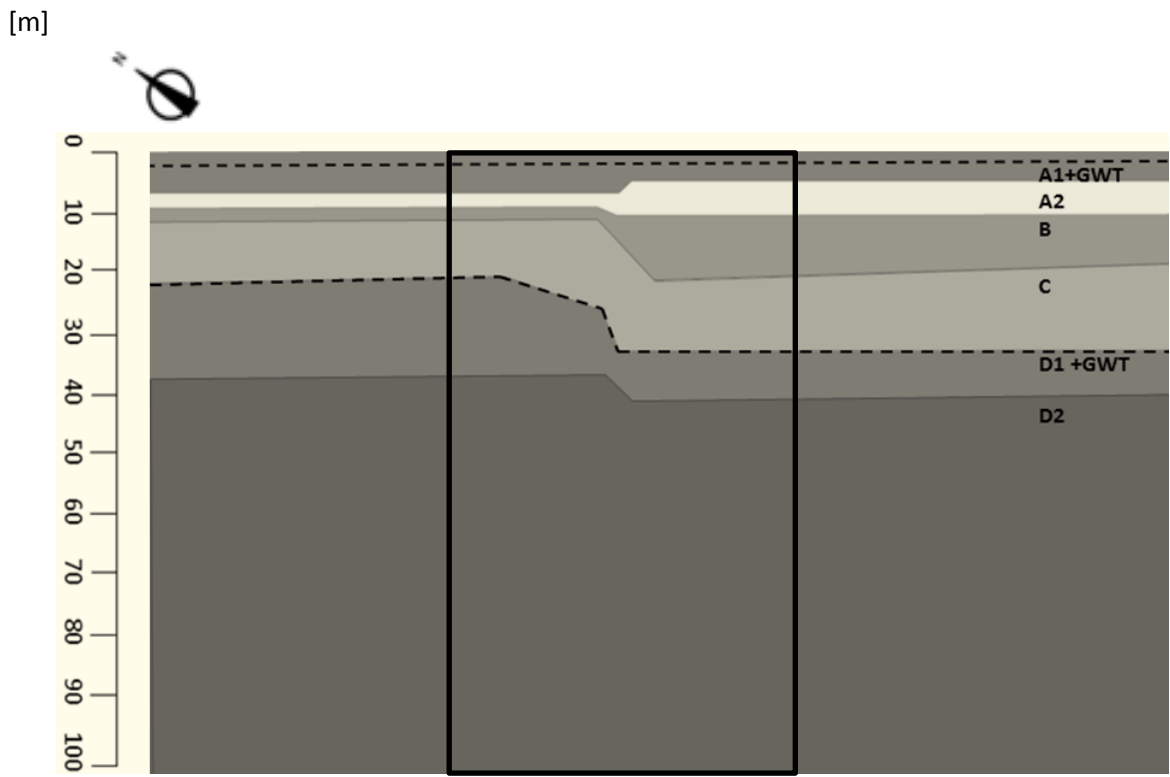


Figure.7. Geotechnical profile defined from the 3D model based on the location of the borehole cross section A-A figure.6. that includes the information layers depth from boreholes M1, M2, M3, M4, M5 and M6 layout B &HAG, 2012

5. Trial shaft construction design aspects

As it has been mentioned on previous sections, the protection of the underground water is the first and most important consideration for any works taken place in the area where the train station is located.

The prevention of a possible bridging of contaminants into the artesian reservoir is a must,(see figure.4f.). Other considerations like the mechanical properties of the soil layers found were also considered for the final design that was constructed. The final project included a diaphragm wall with a thickness of 0.8m, with a sacrificial bottom slab jet grouting depth 5m in depth that should act as plug to prevent the contamination of the artesian aquifer, and at the same time act a structural support for the D-walls at the bottom of the excavation. The shaft was set to have a final excavation level of -18m. The diaphragm

walls were done by panels with a depth of 24 m (See figure.9.), The walls of the shaft are internally supported by the use of Walers and trusts using HEB 300 steel profiles.

5.1. Design failure

After the second and third level of the excavation was reached a series of events took place, showing that the given design for the support was not sufficient. A set of extra supports where used in order to avoid the collapse of the shaft.

In this study the supports used for the numerical modelling will follow the first study that was done where the use of a 2D analysis program provides information about the existing pressures and the necessary support. Antri,(2015).

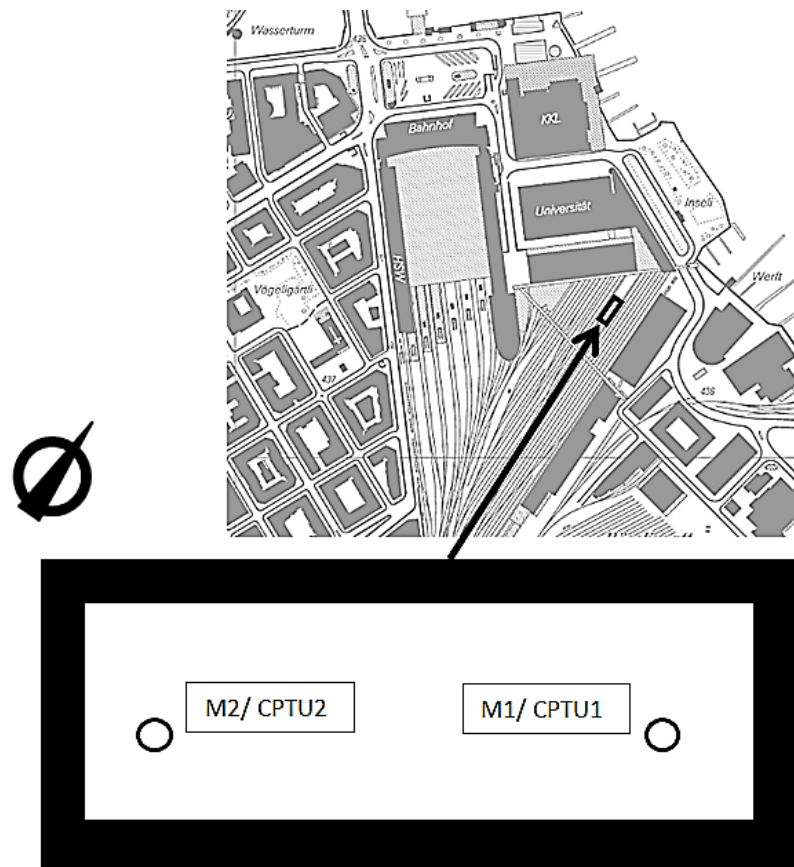


Figure.8. Lucerne central station, trial shaft. It is possible to see the shaft is located between the right hand side hand and in the vicinity of one of the buildings part of Lucerne University.

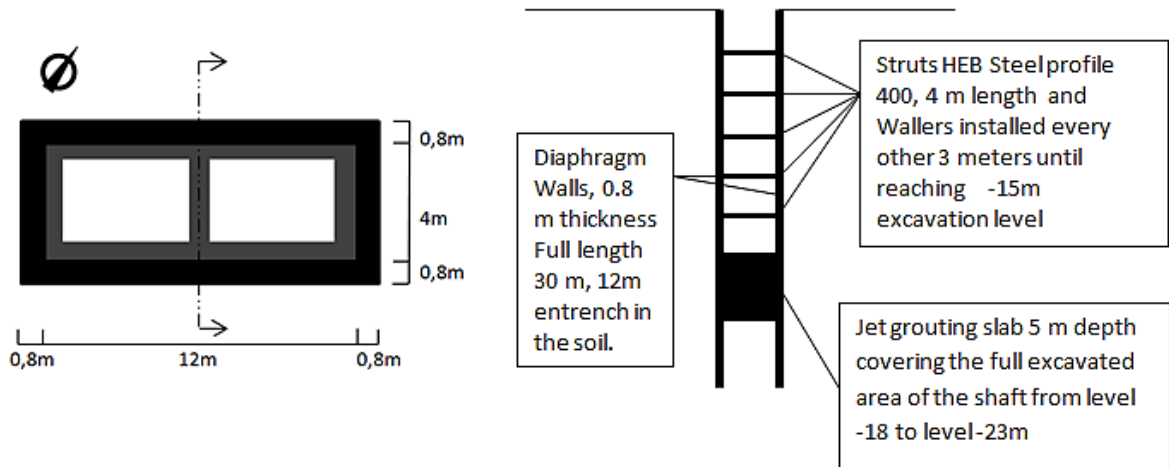


Figure.9. Trial shaft structural elements, where the steel struts and the spacing of 3 meter is different from the original design as well as the type of HEB profile. The present structural design comes after the first study using 2D analysis Anti, 2015.

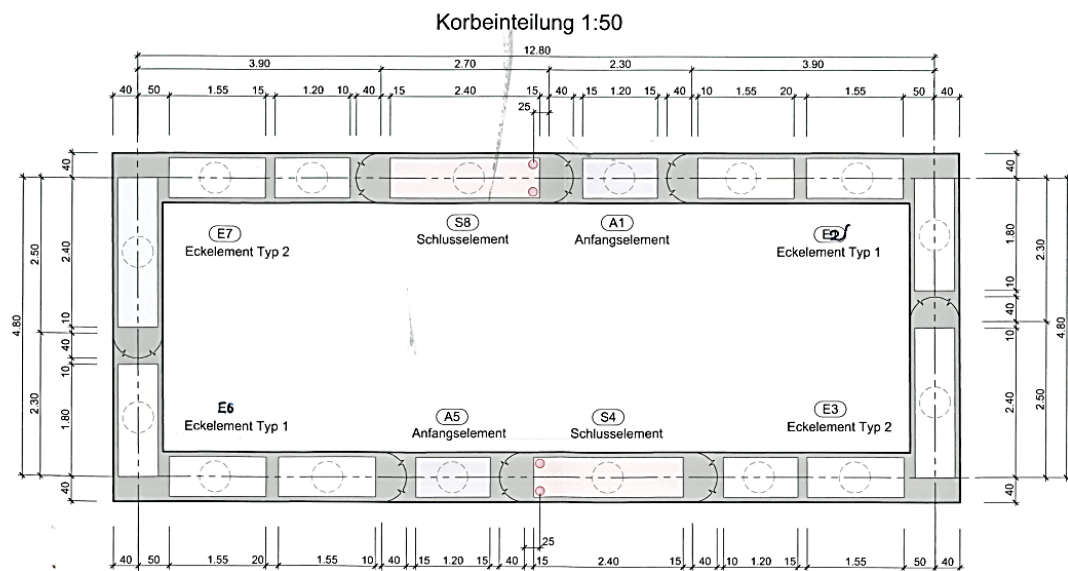


Figure.10. Lucerne Central station Trial shaft construction floor plan where the location of the excavation panels, with their type and dimensions as build.

6. Theory review

6.2 Diaphragm walls design - analytical solutions

Soil retaining structures are designed to support the active pressure of the contained soils and surcharge load that could be found next to the excavation they served to protect, transmitting the horizontal loads to the soils found at the bottom of the excavation. The intention in all design proposals is to find the equilibrium between the adjacent soils and the retaining structure.

Among the common checks on the design of diaphragm walls are:

- The stability of the horizontal loads.
- The stability of the retaining system (D-Wall), in case of a soil failure.
- The stability of the structural support system (Struts, Wallers, anchors, etc.).
- The stability of the bottom of the excavation that could be compromised due to excess of pore pressure.

A summary of the method for the calculation of D walls has been done by Delattre (2001) where it is possible to see the categorization of the methods in 5 distinct approaches lines. (See figure.11.).

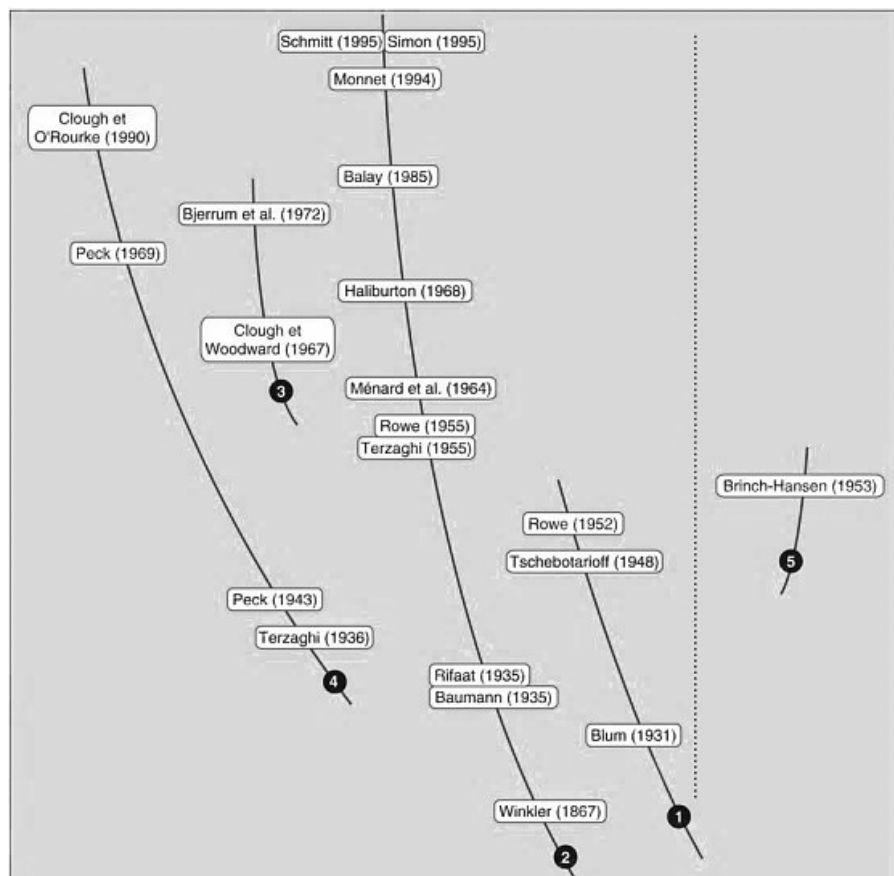


figure.11. five distinctive analysis approaches to diaphragm wall design (Delattre, 2001)

Table. 7. Design classification in accordance with delattre approach lines summary 2001

Diaphragm walls design methods – Classification		
Method line in accordance with figure.8.	Type	Comments
Blum	Classic method	Referential or fully empirical in nature
Winkler	Soil reaction method	Analytical method based on elastic analysis
Clough	Finite element method	Numerical methods where the use of computer is a must due to the large amount of calculations
Terzaghi	Empirical methods	Base on observational method
Brinch Hansen	Ultimate limit state analysis	Semi-empirical method

Empirical methods

This method has been used traditionally in the past especially when it comes to foundation design and underground constructions proving to be considerably valuable in geotechnics. Some construction codes for the dimensioning of foundations and retaining structures in Germany and the United States, have taken these methods as the base for their standards when it comes to determine the pressure distribution along the wall as well as for the derivation of wall deformations and associated adjacent soil movements due to the construction of the D walls and the excavations.

Semi-empirical methods

These methods combine the observed behavior of constructed D walls along with Limit equilibrium analysis that is adjusted to the observed behavior of retaining walls. The methods have been quite popular in Germany as well as in the United States, where construction research institutions have created a large data bank from where extraction and analysis of the behavior of D-walls in different kind of soils has guide the establishment of recommendations and guide lines for the design and execution of diaphragm walls as per regions. In any case, the semi-empirical methods does not provide basis for a generalized solution as they are based on observation on a particular area where soil layer and weathering process are of a particular nature and therefore cannot be used as a case for a rule.

In 1936 and 1943 Terzaghi, has studied the case of unloading of the retained soil considering whether the movements of the D-wall takes place at the toe of the wall, or from the upper part or if it is a generalized movement of the whole wall. This method was used in the United States and Germany, where it was further developed between 1940 -1980 by German engineers such, Press, (1942), Briske, (1952), Briske (1958), Müller – Haude and Scheibner, (1965), Schmitt and Breth, (1975), Briske, (1980) has done scale models to simulated the behavior of D –Walls studing the earth pressure distribution in the trasdos of the Diaphragm wall as considering the stiffness of the wall and the location of the structural

support such as struts and walers, the medialization results were then validated by contrasting with on-site measurements of deep excavation works in different type of conditions in different cities in Germany.

In 1975 Weissenbach, has performed a validation of this analysis and has written 3 volumes where all this results are presented with their corresponding analysis. This work has served as the basis for the national guide lines found in (Empfehlungen des Arbeitskreises Baugruben) for retaining structures and in the EAU (Empfehlungen des Arbeitskreis Ufereinfassungen), (See figure.12).

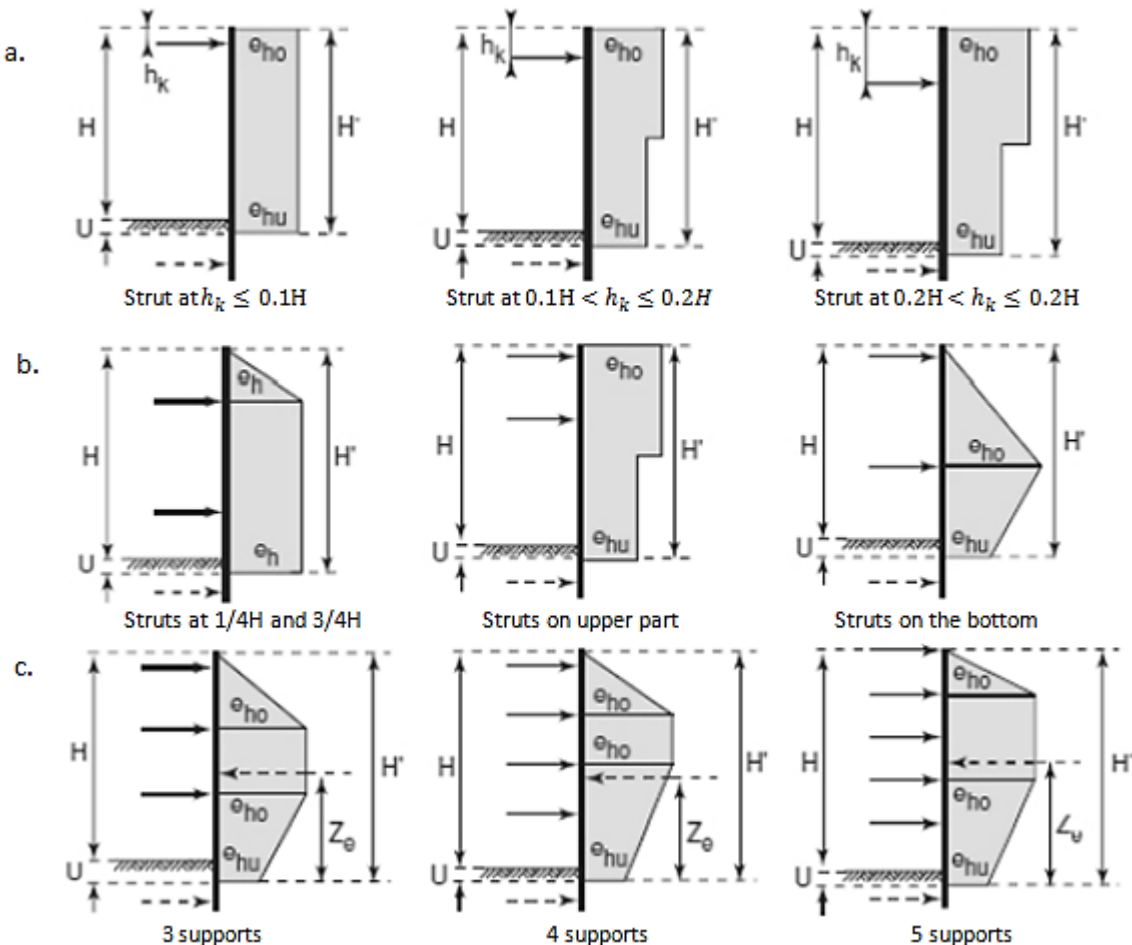


Figure.12. Briefing of the German guidelines EAB for earth pressure redistribution considering the location of the lateral supports and the number of them. a. EB 70-1 D -wall lateral earth pressure redistribution; b. EB 70-2 D- wall lateral earth pressure redistribution with two supports, c. D- wall lateral earth pressure redistribution with three or more lateral supports

Analytical methods

The analytical approach has been developed using simplified models to complex numerical methods. During 1930 the classic methods of D-wall design were developed at a time where the design was fully done by hand calculations and the use of tables. In a later state of

the analytical method development, from 1970 the advancement of computers enhanced the development of new numerical methods, which numerical processing was more intensive. Now days, with the exponential development of computer processors and the expansion of the use of computers in the engineering field, the use of finite element method has become quite popular, considering that if the assumptions, simplifications and design approach are correct, the results can proof to be close to the actual soil-structure interaction.

The classical methods base the estimation of stability and therefore does not defined the possible displacements of the wall. In order to obtain the displacement of the wall the methods of soil responds or ballast module or (Sulzberger ratio), that was studied in depth by Terzaghi. This parameter associates the transmission of stresses to the soil by a stiff plate with the deformation of the soil as it penetrates the same soil. In other words, is the ratio of the slope of the line that joins the origin of coordinates with the point in the curve of stress – strain that is generated plate (See figure.13.)

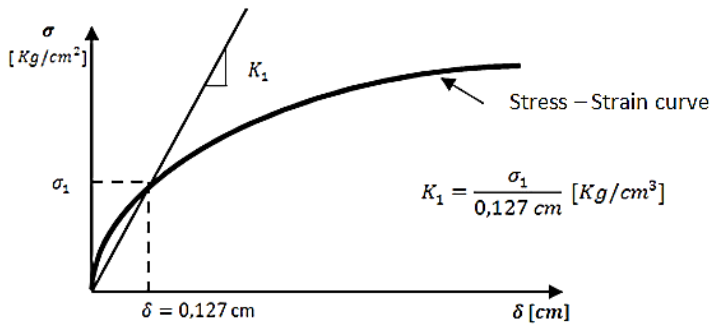


Figure.13. Stress-strain curve and ballast moduli

The use of finite element analysis also provides an approximation on the D-wall displacements and possible deflection.

Three main groups of D-walls approaches can be identify. The classical methods, the elastic methods and the numerical methods.

Limit equilibrium method

As a part of the group of classical methods, this method is based on the limit equilibrium of the soil considering that the lateral earth pressure apart from the possible deformations caused in the retaining structure. It is also assumed that the displacements of the D-wall are sufficient to reach the equilibrium state within the excavation.

The most common used theories in the group of classical methods are the Coulomb for granular soils and Rankine for clay materials.

The Blum method hypothesis assumes that the summation of moments and forces acting on the D-all in relation to the pivot point is cero. The method considers that the D-wall rotates around a point located above the bottom part generating a law of passive and active earth pressures (See figure.14.). In order to simplify the calculation procedure, the earth pressures

found under the pivot point are replaced by a resultant force R, applied at the same point where the earth pressure where at first found. (See figure.15.)

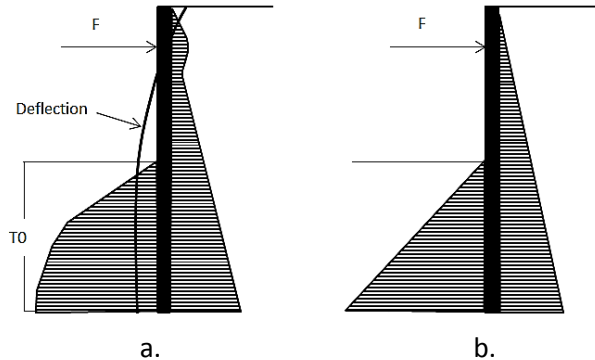


Figure.14. Behaviour of a D-wall supported in the upper part of the wall under equilibrium. a. Wall deflection due to active earth pressure; b. D-wall under equilibrium assumption

Other method such as the european method, where part of the passive earth pressure in the intrados of the D-wall is considered provides a maring of safety. In this method it is assumed that there is no point of rotation as that the wall is supported at two points, one in the upper part and the other at the level where the wall is going into the soil. This method follows the Blum method calculation with the only difference that in this case the nature of the analysis is hyperstatic requiring an aditional assumptions and a more extensive calculation. The assumption consist in having cero bending moments due to the active earth pressure. This assumption could only be use with homogenous and granular soils. (See figure.12.)

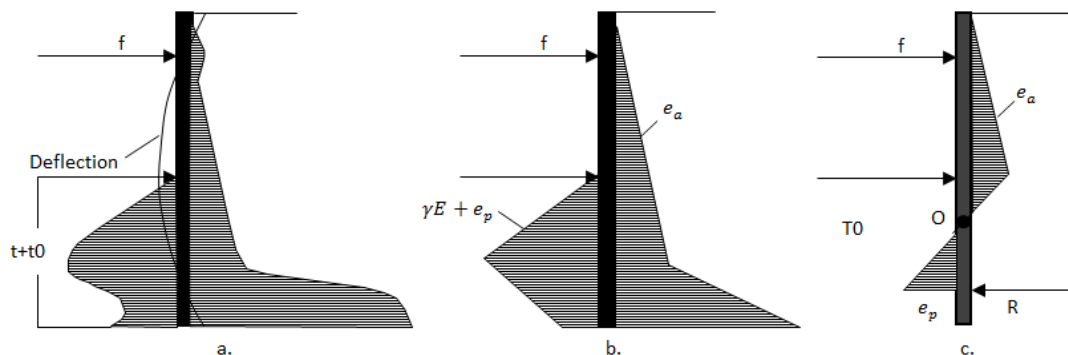


Figure.15.D-wall analysis considering the wall supported in two points. A. Bending and passive and active earth pressures; b. Active and passive earth pressure simplified scheme; c Scheme under equilibrium assumption

D-wall supported with multiple struts

In the case where the D-wall is supported at different levels, the depth at which the wall is embedded in the soil should be check for the full stability of the wall. The main assumption in this case, is the displacement of the passive earth pressure where the wall is embedded (See figure.17.).

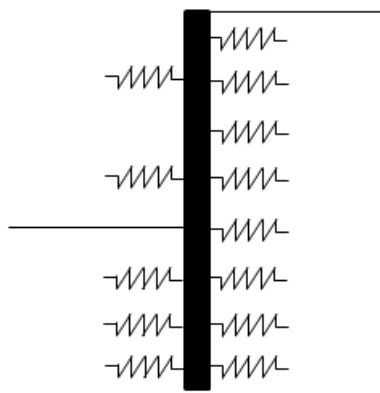


Figure.16. D-wall behavior considering several supports.

For this method Caquot (1937) proposed to take advantage of the stiffness of the D-wall by installing the supports at the levels where the reaction were equal in order to maintain the equilibrium of the system and therefore not having a fixed distance between each support level. The distance as the excavation gets near the bottom level decreases. The method can be used in soils with different conditions (See figure.17.)

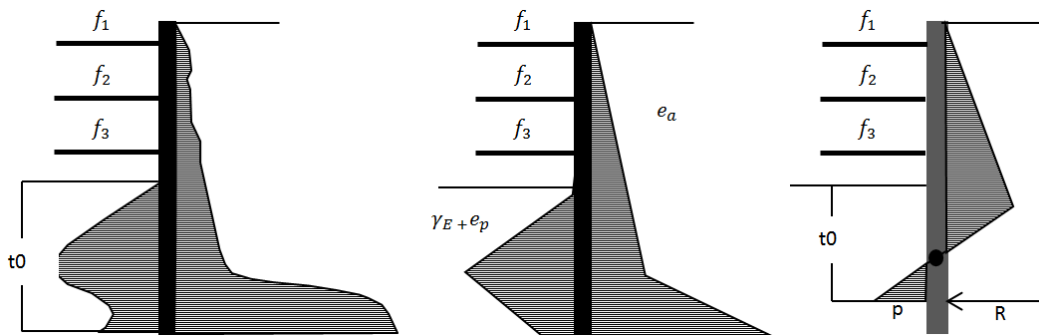


Figure.17.D-wall under equilibrium using several support levels. a. Active and passive earth pressures; b. Simplified earth pressure; c.D-wall with several support levels in equilibrium.

Magnel, (1948) proposed a calculation procedure where by making some assumptions a simplified method is derived. This method yields some conservative results due to the simplification. The assumptions and considerations are as follow :

- To consider the D-wall as a supported beam where the passive earth pressure has an importance on how the wall behaves.
- To assume a fictitious support under the bottom of the excavation.
- To assume that the passive earth pressure will be two times the active earth pressure.
- To not take into account the friction angle from the soil to the D-wall nor the cohesion of the soil.

Elastic methods

The elastic methods consider the soil-structure interaction and therefore the soil deformation parameters, the contribution of the D-wall stiffness to the equilibrium of the system, and the possible displacement that could take place. The most common are those methods that consider the reaction of the soil using the sprint model. In order to obtain the ballast moduli a set of results from a presiometer are a must.

The use of the ballast moduli is also known the subgrade method and also as the Winkler method, as in 1867 Winkler introduced the use of subgrade moduli to his elasticity theory that served as the base for further studies performed by Zimmermann, 1988. These studies lead to the first applications of the soil-structure reaction method to calculated stresses produced by the train tracks on the sub base soil. From this later study the name of Ballast method or ballast ratio has been mainly known. Later on, Baumann and Rifaat, 1935 introduced the use the method to the design of D-walls. Years later, Boudier, 1970, Fages and Boyat 1971, and Rosignol and Genin,(See figure.16.)

7. The Finite element method

Numerical methods have been used in the analysis of structure-soil interaction providing reliable results when calculating / forecasting the reaction between structures and soils in cases where the analytical solutions are limited. It is possible to consider the use of FEM as extra-polarization of matricial calculation for the analysis of structural beams of a continuous type. Prior the use of FEM during the beginning of 1940 the first attempts to solve 2 dimensional elasticity problems using matricial methods dividing the continuous beam into elements took place Mc Henry, D. (1943).

The finite element method considers in its application in geotechnics and as for this study, of D-wall analysis, the soil as a discretized continuum, therefore, it takes into account the interaction of the wall and the soil in both intra and extrados of the wall.

The main issues when using FEM are the collection of data necessary to represent the soil layers are found on site, as well as the lack of precision when representing the existing conditions e.g. tridimensional geometry, corner effects, etc. The used codes in most cases require parameters that are complex and that sometimes do not have a define representation in reality.

In geotechnics the analysis is done by integrating the continuum soil-structure in a mesh usually made of triangles with nodes that represent a given degree of freedom corresponding to the possible deformations, displacements to be calculated. Bringkreve et al, (2002).

7.1. Development of FEM

In 1943 Curant, R., presents the concept of continue element, by solving plane elasticity problems by dividing the domain of analysis in triangular elements onto which a polynomial variation was assumed.

In 1960 Clough, R.W, present his work on the solution of plane elasticity, the finite element method, suggesting the denomination of finite elements. Since that date until now, the FEM has crossed through an important development presenting its benefits in the solution of plain elasticity in a wide range of fields, ranging from structural engineering, geotechnics, and medicine. This exponential development has been also assisted by the development of computers.

From the perspective of the design and analysis of geotechnical works such as excavations, shafts, tunnels, foundations and slope stabilization problems, the most attractive feature of the FEM, is the most dangerous one as the FEM is an approximation method.

FEM should be included as a part of the set of tools without letting aside the analytical approach. FEM is a tool and should not be treated as a paradigm, the method, provides useful information about the behavior of complex structures, for which an analytical solution does not exist but it could also lead to important failures.

For the case of the present study, the trial shaft in Lucerne, there is a group of singularities that are to be considered:

- The differences in level of the soil layers and the complex geometry that this represents.
- The nonlinear behavior of the soils
- The use of multiple hypotheses for the calculation, e.g. overburden loads, differential settlements, slips, cracking of structural elements among others.

Is therefore, the FEM a basic tool in the resolution and analysis of complex problems providing the capacity to model complex geometries that could be done in 2D as a simplified model or if necessary in 3D. The FEM gives the option of prescribing displacements, the use of advanced constitutive equations, the possibility to handle large numerical calculations necessary in order to analyse nonlinear dynamic and static problems.

It is also possible to run the numerical analysis on sub models to obtain localized behaviour results.

7.2. 3D finite element analysis

Following the above explanations regarding FEM, there are situations and projects where the mechanical, geometrical or loading characteristics do not allow the use of simplified calculation methods, as in the case of a two-dimensional or rotational solid. The beam elements, plates or shells. For such cases it is a must to conduct a tridimensional analysis (See figure.18.)

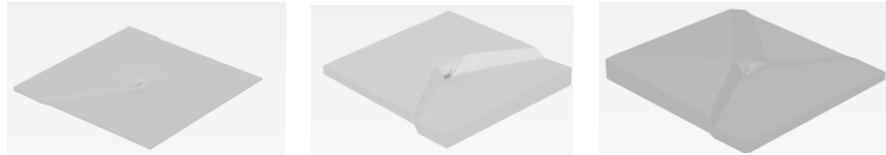


Figure 18. Plaxis 3D models showing the complex geometry of the model due to the changes of soil layer levels. The area where the shaft is located presents a complex geometry that represents different active earth pressures at the same level on the D wall.

7.2.1. Finite element analysis using 3D modelling

Displacement space

If a 3D body is analyzed the movement of one point in the given 3D space is defined by three vector components of displacement.

$$U = [u, v, w]^T \quad (1)$$

Where u, v, w represent the displacements at a given point in the Cartesian coordinate system x, y, z accordingly.

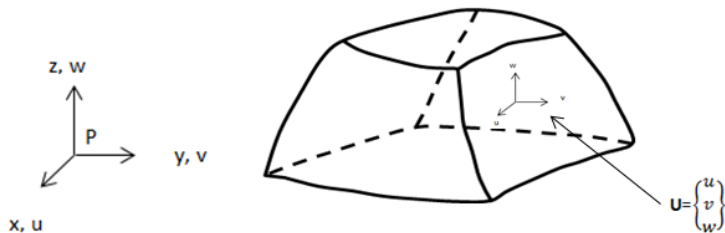


Figure 19. Tridimensional case where the displacement vectors of a point are shown Timoshenko, (1968)

Strain field

Based on the classic theory of tridimensional elasticity by Timoshenko, S.P and Goodier, J.N 1968), the deformation vector in a given point is determined by six components.

$$\varepsilon_x = \frac{\partial u}{\partial x}; \quad \varepsilon_y = \frac{\partial v}{\partial y}; \quad \varepsilon_z = \frac{\partial w}{\partial z} \quad (2)$$

$$\gamma_{xy} = \frac{\partial u}{\partial y} + \frac{\partial v}{\partial x}; \quad \gamma_{xz} = \frac{\partial u}{\partial z} + \frac{\partial w}{\partial x}; \quad \gamma_{yz} = \frac{\partial v}{\partial z} + \frac{\partial w}{\partial y} \quad (3)$$

Where: $\varepsilon_x, \varepsilon_y, \varepsilon_z$ are the normal deformations and $\gamma_{xy}, \gamma_{xz}, \gamma_{yz}$ are the tangential deformations.

Stress field

The stress vector in a given point of a 3D solid has six stress components, as a result of the respective deformations, therefore.

$$\sigma = [\sigma_x, \sigma_y, \sigma_z, \tau_{xy}, \tau_{xz}, \tau_{yz}]^T \quad (4)$$

Where: $\sigma_x, \sigma_y, \sigma_z$ are the normal stresses and $\tau_{xy}, \tau_{xz}, \tau_{yz}$ are the tangential stresses. (See figure.17.)

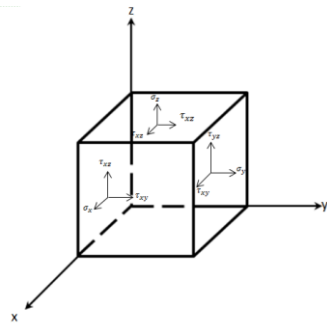


Figure.20. Stresses direction in a tridimensional solid
Plaxis material manual (2011).

Strain stress correlation

The relation of the six strain and stresses in a 3D solid is expressed in a general form of anisotropic elasticity, by the use of a symmetrical matrix 6x6 with 21 independent coefficients. As for the case of orthotropic material, the number of coefficients is reduced to 9. Lekhnitskii, S.G.(1963).

It is important to mention, a common case of isotropic elasticity, where the independent coefficients part of the constitutive equation are reduced to 2, the young modulus of elasticity E and the Poisson ratio ν .

In general it's possible to say that the behavior of 3D solids and 2D plate elements is similar. Therefore the hexahedrons provide pre precision than the tetrahedrons of the same magnitudes.

8. Constitutive model used in numerical analysis of soils

In the regular exercise of numerical modelling, there are two main categories of models that are used to describe the behavior of the soils layers within a given model. There are more models that are at the moment used out of the application field are more used for purpose of academic research. In this paper reference is only done to those models that were used.

The perfect plastic model and those models that consider a hyperbolic function where it is assumed that hardening of the material takes place as the loading due to excavation or activation of surcharge load takes place. These two categories are used in accordance where

the designer is interested to observe with more detail the behavior of a given layer. It is also worth it to say that this models can be used in all layers of the model but it should also be considered that for those hyperbolic models a larger amount of information is required, and the use of values found in tables can bring deviation from the model results and the real soil behavior of the structure or excavation. In this study and as a variance from the first study by Antri, 2015, all layers will be analyzed using HS-ss model or M-C model parameters but not combined.

8.1. Mohr Coulomb model

The Mohr Coulomb model is based on the elastic perfect plastic assumption. In the analysis of geotechnical works this model is used as a first approach to the analysis of soil behavior in a general form, where it is possible to see a possible path within the stress distribution in terms of stress directions and main plastic points describing a possible failure mechanism. It is also used on the modeling of granular loose soils or fine soil materials that are found to be normally consolidated. It is also important to mention that M-C model does not represent the progressive elastoplastic behavior of the soil, but as mentioned before it follows an associate elastic perfectly plastic law that is related to plastic deformations. (See figure.18.).

The M-C model uses five parameters that are commonly used by most practitioner engineers as they do not need any specialized testing and in some cases even extracted from existing tables as a guide values to determine in the first stage of a design the possible behavior of the soils studied. Young's modulus E , Poisson ratio ν , Cohesion C , Friction angle φ , and dilatancy angle ψ .

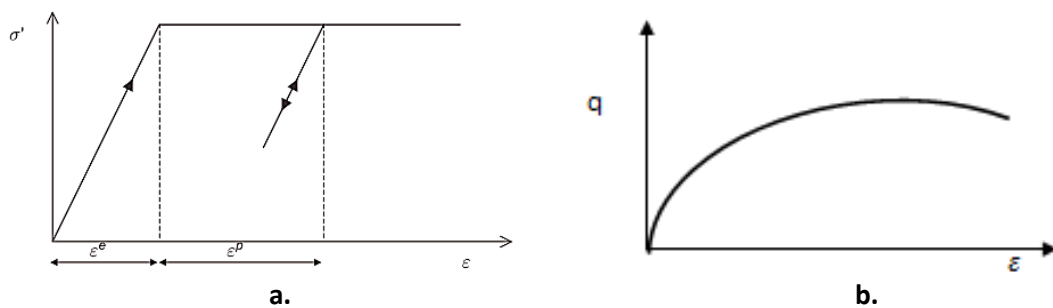


Figure.21. a. Elastic perfectly plastic mode (Plaxis material manual 2011); b. Triaxial drainage test soil behavior

In the M-C method plasticity is evaluated by including a flow rule that serves to define the beginning of the plastic response and the end of elastic behavior of the soil material. (See figure.21.).

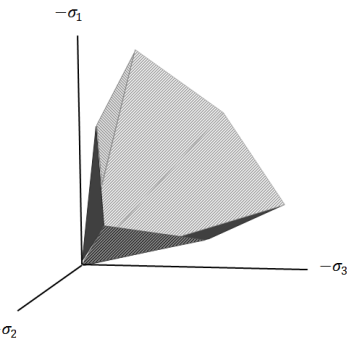


Figure.22.Mohr-Coulomb failure surfaces in the principal stresses space (PLAXIS material manual 2011)

Mohr-Coulomb model include, as mentioned before, a flow rule that defined the limit of elasticity and plasticity phases of the modelled soil material behavior. As shown in figure 19. The graphic representation of such flow rule is done by using a hexagonal cone in the principal stresses space, with surface of fixed flow. Considering that all the possible inscribed points within the yield surface represent an elastic behavior of the material. At the point where the stress reaches or cross the fixed flow surface, it is said that elastic as well as plastic deformation has taken place.

The mentioned flow rule is a representation of the friction law of Coulomb for the general analysis of principal stresses. This model have some limitations as it cannot included the increment of stiffness that if found with depth, as it does not include the stiffness dependency with the stresses nor the path described by the dependency of the stiffness with the stresses.

8.2. Hardening Soil model

The hardening Soil model uses the same parameters as in the M-C model to describe the limit state, the friction angle, the apparent cohesion and the angle of dilatancy. The Hardening soil (HS model) requires more inputs as in the M-C. In this second method as its name suggested the soils will undergo a process of hardening by incrementing the stiffness of the material as the loading process take place. The stiffness of the soil is therefore describe in a more accurate form by introducing three stiffness parameters such as the stiffness at 50% of the maximal stiffness before collapse, E_{50} , the stiffness during unloading –reloading during triaxial testing $E_{ur} \approx 3E_{50}$ and the stiffness due to loading when performing the odometer test $E_{oed} \approx E_{50}$. (See figure.20.a.b.).

The mentioned parameters can be calculated by using the following equations accordingly, whereas the minor principal stress σ'_3 degrades the stiffness degrades. In Plaxis 2D and 3D a value of 100 KPa is used as a default value.

$$E_{ur} = E_{ur}^{ref} \cdot \left(\frac{c \cdot \cos \varphi - \sigma'_3 \cdot \sin \varphi}{c \cdot \cos \varphi + p^{ref} \cdot \sin \varphi} \right)^m \quad (5)$$

$$E_{50} = \left(\frac{c \cdot \cos \varphi - \sigma'_3 \cdot \sin \varphi}{c \cdot \cos \varphi + p^{ref} \cdot \sin \varphi} \right)^m \quad (6)$$

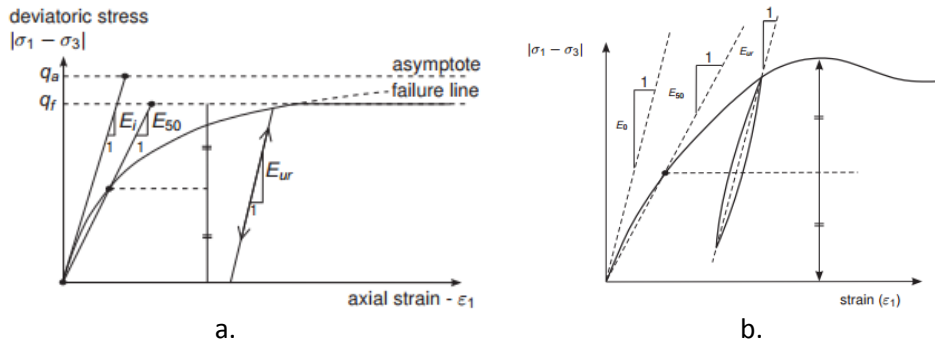


Figure.23.a Hardening soil hyperbolic stress-strain relation during primary loading, Duncan –Chang model b. Definition of E_0 , E_{50} , E_{ur} , (Plaxis material manual, 2011).

H-S model is a variant of the hyperbolic model, that where mention at the beginning of this section on constitutive models. The new part about this model is the introduction of the effects of compression, hardening, that simulated the irreversible compaction of soil materials under a primary loading condition.

The model can be used to simulate the behavior of soft soils (clay like materials) as well as grain materials (sand and gravels). The flow rule in this model is not confined to the principal stresses space as it is allow it to expand with the associated plastic deformations and as a function of the stresses found in the material before loading is considered.

It is also relevant to mention the importance of the two elements that the H-S model introduces to the numerical analysis, that serve as a reference of the changes in stiffness in given model soil material. The hardening due to friction that is present in soils undergoing a plastic phase, (friction hardening) and the irreversible compaction due to a primary loading (compression) that is located in the cap of the model the so called hardening cap. (See figure.24.).

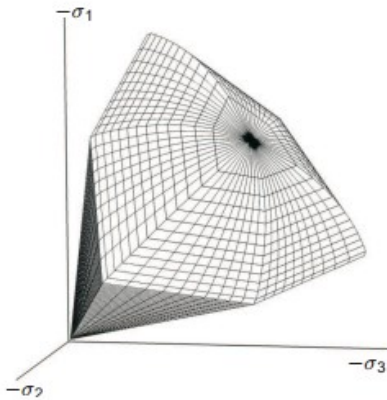


Figure.24. representation of total yield contour of Hardening soil model in the principal stress space for cohesion less soil
Plaxis material manual, 2011.

The basic formulation of the model can be explained as the hyperbolic relation that is usually observed during triaxial test between the axial vertical deformation ε_1 and the deviatoric stress $|\sigma_1 - \sigma_3|$ (See figure.20.a). The HS takes into consideration the dependency of the stiffness strain modulus, in this form, the stiffness is increments with the applied pressure. The H-S is limited in the sense that it does not consider the softening of the soil material due to the dilatancy that takes place as the soil particles, after been compacted, start rolling over each other undergoing into a softening phase due to the dilatancy.

Advance parameters for Hardening soil model

Apart from the mentioned parameters, the Poisson ratio for unloading and reloading ν_{ur} , is included in the materials parameters.

8.3 Hardening Soil with small strains.

This model is a variation of the previous model H-S, that takes into consideration the stiffness of the soil but in short deformation steps (small strains). By using small strains the soil material exhibit a non-linear increment of the stiffness. This is done by introducing three new parameters to the numerical analysis to those mentioned in the section of Hardening Soil (HS). The shear module with small strains G_0^{ref} , Shear modulus with small strains ($\varepsilon < 10 - 6$) and $\gamma_{0.7}$ that expresses the shear deformation modulus been reduced to 70%. In the same form as the Hardening Soil model, the HS-ss does not consider the softening of the soil due to dilatancy and the power for stress level dependency of stiffness m (See figure.25.)

The relation of the small-strain shear modulus G_0^{ref} , and the reduction of the secant modulus $\gamma_{0.7}$, is expressed according to Hardind & Dmevich (1972), using the following equation

$$\frac{G_s}{G_0} = \frac{1}{1 + \frac{3}{7} \cdot \left| \frac{\gamma}{\gamma_{0,7}} \right|} \quad (7)$$

Where $a = 0,385$

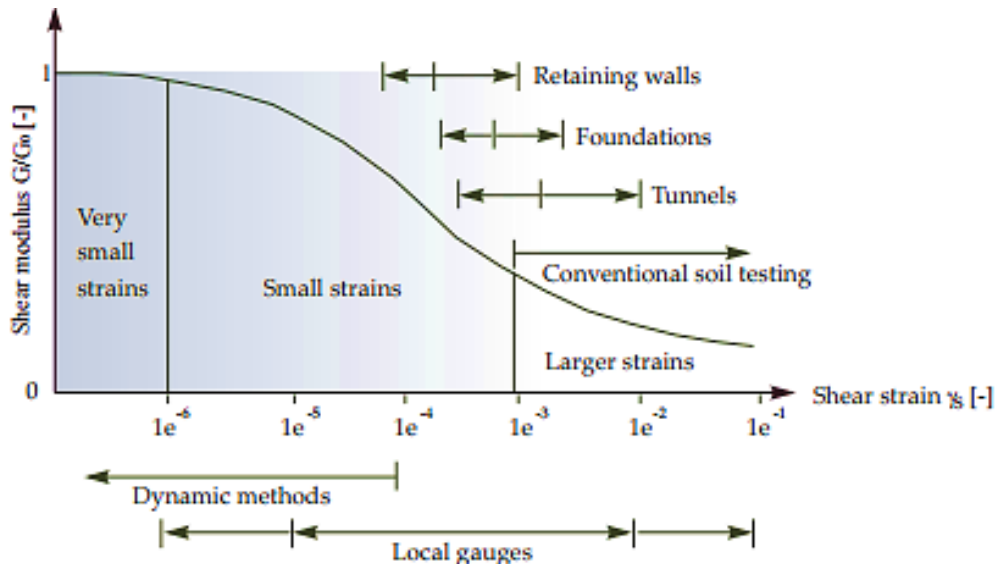


Figure 25. Characteristic stiffness-strain behavior of soil with typical strain ranges for laboratory test and structures (after Atkinson & Sallfors, 1991)

8.4. Linear elastic model

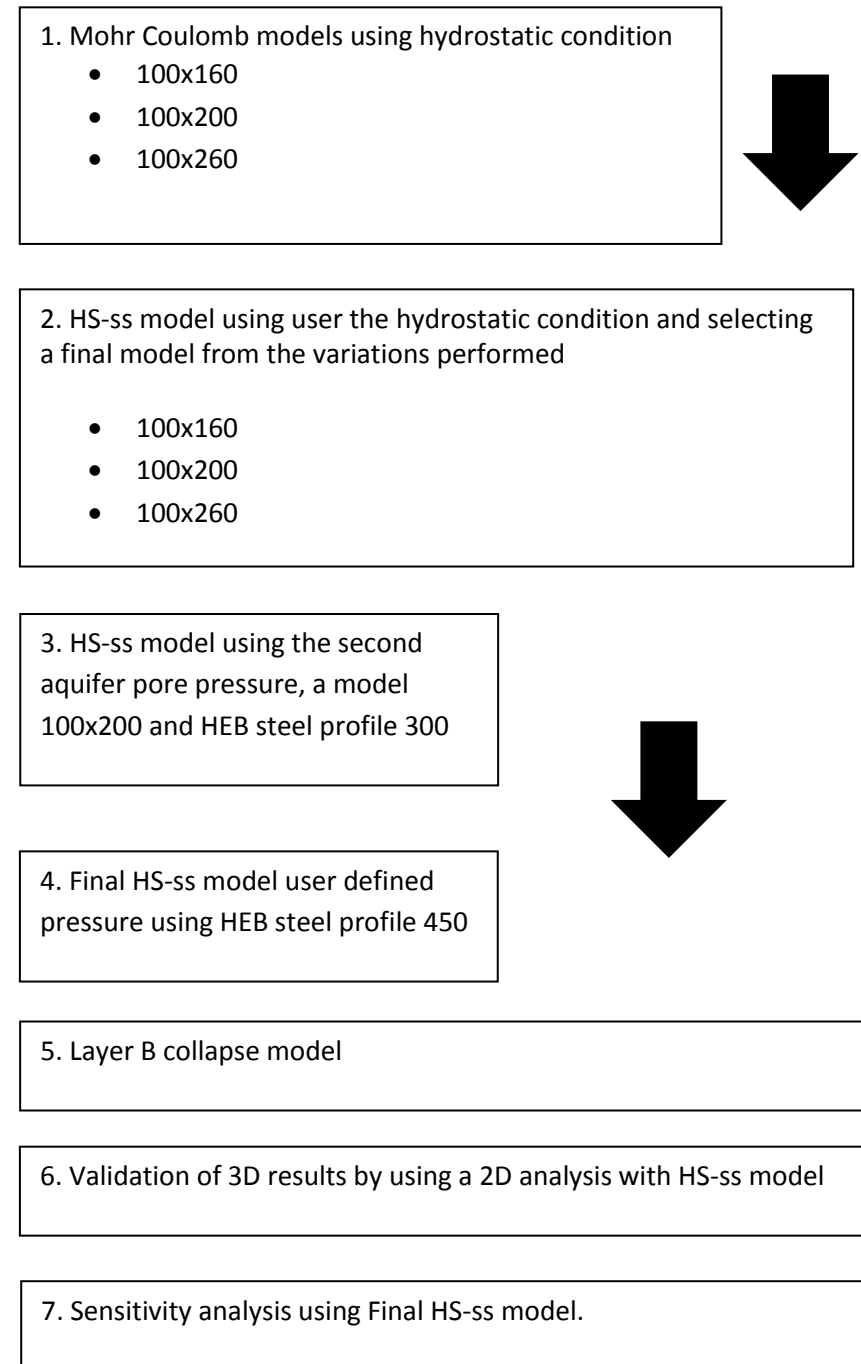
This model is used for over consolidated clays and some rocks with that can undergo under a large elastic phase. Apart from these cases, it is usually used for structural elements where the Hooke law of linear isotropic elasticity can assist on the calculation of bending and flexural deformations. The model includes parameters such as the Young modulus, E, and the Poisson ratio, ν . These model present lots of limitations for the simulation of soils. Is mainly used for structural elements, beam, plates, and anchors.

Preliminary remarks about Plaxis numerical modelling

The numerical analysis will be done in accordance with the next task flow chart.

It is relevant to mention that the differences between the hydrostatic model using the head pressure that is included when creating the layers, has a very small impact on the results if the head pressure is used or if the head pressure is used and the user defined option, PLAXIS AE 3D has shortened the calculation of pore pressure by allowing the user to include this by using the user define option, when creating the soils layers. The same could be done in the flow conditions section, in the case the layers are at the same level and therefore a reference head can be included.

9. Modelling work flow



9.1. Model parameters

The geotechnical profile used is obtained using the information of boreholes M6, M2, M1, M3 and M4 and M9 the shaft configurations, strut levels and dimensions are the same as where used in the previous study. Antri,(2015). (See figure.26b)

Geotechnical parameters

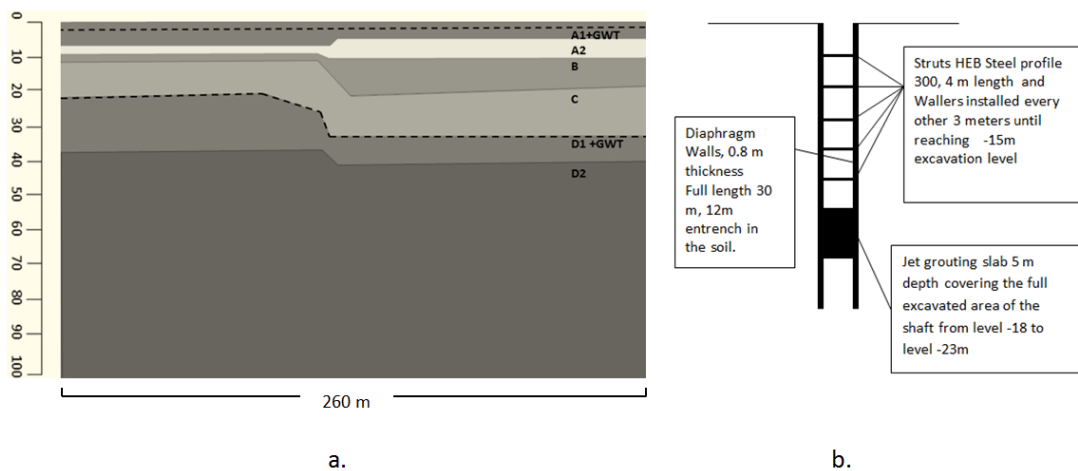


Figure.26. a. Geotechnical section used for numerical analysis; b. design details part of the model in 2D and 3D.

Table.8. Model parameters based on borehole M2 material properties for M-C model drained condition.

Soil ID	γ_{unsat}	γ_{sat}	E'	φ	v	c'_{ref}	k_v	k_h
	[kN/m ³]	[kN/m ³]	[kN/m ²]	[°]		[kPa]	[m/d]	[m/d]
A1	20	20.5	6000	28	0,3	1	0.864	0.864
A2	18.5	19	4500	34	0,3	0.1	0.000864	0.0432
B	20.5	21	8000	26	0,3	0.1	4.32	4.32
C	18	18.5	2700	24	0,3	0.1	0.000864	0.00864
D1	19.5	20	5900	27	0,3	0.1	0.864	0.864
D2	19.5	20	3800	30	0,3	0.1	0.0432	0.0432

Table.9. Model parameters based on borehole M4 and M9 material properties for HS-ss model drained condition.

Soil ID	γ_{unsa}	γ_{sat}	φ	E_{50}^{ref}	E_{oed}^{ref}	E_{ur}^{ref}	Power	G_0^{ref}	$\gamma_{0.7}$	c'_{ref}	k_v	k_h
t	[kN/m ³]	[kN/m ³]	[°]	[kN/m ³]	[kN/m ²]	[kN/2]	[m]	[kN/m ²]		[kPa]	[m/d]	[m/d]
A1	20	20.5	28	6000	6000	24000	0,7	50000	0,00031	1	0.864	0.864
A2	18.5	19	34	5900	4500	19000	0,9	31000	0,0003	0.1	0.000864	0.0432
B	20.5	21	26	8000	8000	32000	0,5	60000	0,00024	0.1	4.32	4.32
C	18	18.5	24	5630	2700	23657	1,0	38500	0,0002	0.1	0.000864	0.00864
D1	19.5	20	27	109973	5900	43714	0,5	101000	0,00025	0.1	0.864	0.864
D2	19.5	20	30	5478	3800	18617	0,5	103500	0,00023	0.1	0.0432	0.0432

Note: (See appendix.C). for relation of $\gamma_{0.7}$ values, Antri 2015.

Hydrogeological parameters – pore pressure in accordance data from borehole CPTU 1 and 2.

It is also important to mention from the study by Anthi (2015), that the underground water conditions for the model are given by considering the long term behavior of the soils, as well as the analysis by considering the recommendations by Vermeer and Meier (1998), where it was considered to revise which hydraulic conditions were prevalent within the given soil layers based on the consolidation, Terzaghi, (1936)., where the revision of the time factor T_V . must be done. The hydrogeological condition for the modelling part of this report is also done considering that layer C has a low hydraulic conductivity soil layer that serves as a division of the two existing aquifers.

$$T_V = \frac{k_v \cdot M_E}{\gamma_w \cdot D^2} \cdot t \quad (8)$$

Where:

k_v = is the permeability in the vertical axis, M_E = is the corresponding soil stiffness layer B corresponding to D in the equation, t = is the time approximate time that will take the excavation of the shaft. The T_V value is then calculated. (See table.8.)

Considering low T_V values as 0,01 for undrained conditions and $T_V > 0,40$ the time factor.

$$\frac{0,000864 \text{ m/d} \cdot 7430 \text{ kPa}}{\gamma_w \cdot (10m)^2} \cdot 60d = 0,0386$$

The results yields the possibility of considering both cases, undrained and drained conditions, as the value for $T_V = 0,0386$ is in the limit of both hydraulic conditions. In Drained conditions it is known that with time the decrement of shear strength and effective stresses due to the loss of pore pressure in the clay layer will cause a suction force under this layer reducing the passive earth pressure and incrementing the active earth pressure, creating more deformations on the D-wall. Anthi,(2015).

Having two aquifers, a free and an artesian aquifers, PLAXIS provides the option of entering this different pore pressures found at different levels as per borehole, performing the necessary interpolation between the differences in levels given by each bore hole used. The P_{top} and P_{bottom} , of the layers where the second mayor aquifer is found are calculated by using the following equation and inter into the numerical calculation when given the borehole strata levels.

$$P = h \cdot \gamma_w \quad (9)$$

This calculation is done for all the 3 layers that form the aquifer, C, D1 and D2 accordingly and as per borehole. (See table .10.). (See appendix .F).

Table.10. Pore pressure parameters for all the models part of this study.

Borehole material layers summary										
Soil Type	G.W.T	Ground water table using the information from CPTU 1 and 2								
		M6		M2		M3		M1		M4
		Pressure top	Pressure bottom	Pressure top	Pressure bottom	Pressure top	Pressure bottom	Pressure top	Pressure bottom	Pressure top
A1	Free	0	-30	0	-100	0	-10	0	-10	0
A2	Free	-30	-55	-10	-70	-10	-70	-10	-70	-35
B	Free	-55	-70	-70	-180	-70	-180	-70	-180	-50
C	Artesian	-70	-320	-180	-300	-180	-300	-180	-300	-180
D1	Artesian	-320	-370	-300	-400	-300	-400	-300	-400	-180
D2	Artesian	-370	-1000	-400	-1000	-400	-1000	-400	-1000	-360
										-1000

Structural parameters

D - wall material parameters			
γ	D	E₁	v
[kNm ³ /m]	[m]	[kN/m ²]	
24,00	0.80	30,00E3	0.15

Jet grouting slab parameters						
γ_{unsat}	γ_{sat}	E'	v	kv	kh	R
[kN/m ³]	[kN/m ³]	[kPa]		[m/d]	[m/d]	
24	24	1.00E+06	0.2	8.64E-05	8.64E-05	1.00

Struts 300 HEB material parameters					
A	γ	E	I₃	I₂	
[kNm ³ /m]	[m]	[kN/m ²]	m ⁴	m ⁴	
0,01498	78	210E6	0,7989E-3	0,7989E-3	

Waller 300 HEB material parameters					
A	γ	E	I₃	I₂	
[kNm ³ /m]	[m]	[kN/m ²]	m ⁴	m ⁴	
0,01498	78	210E6	0,1172E-3	0,7989E-3	

Struts 450 HEB material parameters				
A	γ	E	I_3	I_2
[kNm ³ /m]		[kN/m ²]	m ⁴	m ⁴
0,0218	78	210E6	0,7989E-3	0,7989E-3
Waller 450 HEB material parameters				
A	γ	E	I_3	I_2
[kNm ³ /m]		[kN/m ²]	m ⁴	m ⁴
0,0218	78	210E6	0,1172E-3	0,7989E-3
Struts 500 HEB material parameters				
A	γ	E	I_3	I_2
[kNm ³ /m]		[kN/m ²]	m ⁴	m ⁴
0,02386	78	210E6	0,7989E-3	0,7989E-3

Mesh parameters

All models are refined in the layers B and C considering that refining these two layers could provide a better approximation for the analysis of the Soft sand layer and the Clay layer and the element distribution is the same in all models following the description in figure.27a.

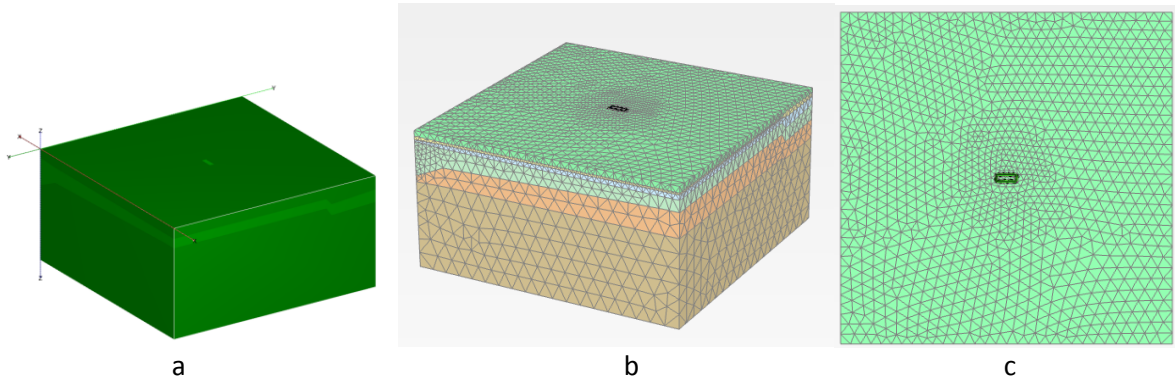


Figure.27. a. Mesh discretization where layers B and C have been locally refined with a 0.5 mesh factor. The volume representing the shaft excavation is refined using a 0.25 mesh factor. The rest of the model has a mesh factor of 0.7.; b. The element distribution is medium. full model view; c. Top view where the medium element distribution is shown

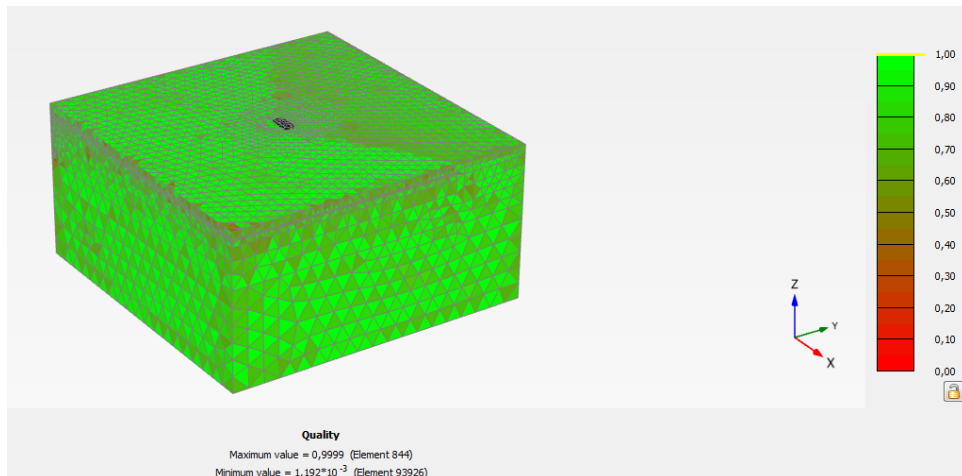


Figure.28. Mesh quality from where it is possible to see the elements distributions, medium.

Calculation steps

The trial shaft calculation is done considering the construction of the D-walls, the construction of the jet grouting slab, followed by 6 excavation levels with the corresponding installation of supports. (Struts and walers). Water conditions selected from the step calculation are hydrostatic mode. This will allow the user defined pore pressure parameters to enter into effect as they are already defined when providing the borehole data to the program. PLAXIS AE 3D, will then perform the analysis considering the difference in level and therefore the difference pore pressure found at different level within the same layer.

Step Number	Name of the calculation step
0	Initial phase
1	D wall construction
2	Activation of interphase
3	Construction Jet grouting slab level -18 , -23
4	Excavation level -3
5	Installation support level -3
6	Excavation level -6
7	Installation support level -6
8	Excavation level -9
9	Installation support level -9
10	Excavation level -12
11	Installation support level -12
12	Excavation level -15
13	Installation support level -15
14	Excavation level -18

Results

The results are presented following the modelling flow chart presented at the beginning of this section. For references on how what this values represents according to the 3D models.

1. M-C model variations results

Table.11. M-C results in accordance with model size variations where the area is change maintaining the same depth of 100m

Last calculation step at -18 m	Measure	Units	100x160	100x200	100x260
	$ U $	[m]	0,1865	0,01884	0,02999
	$ U_y $	[m]	3,840E-3	4,438E-3	4,501E-3
	M_{11}	[KN m/m]	610	184,9	152,1
	Q_{13}	[KN/m]	647	241,6	205,8

Where:

$|U|$ Total displacements; $|U_y|$ Horizontal displacements; M_{11} Bending moments; Q_{13} Shear force

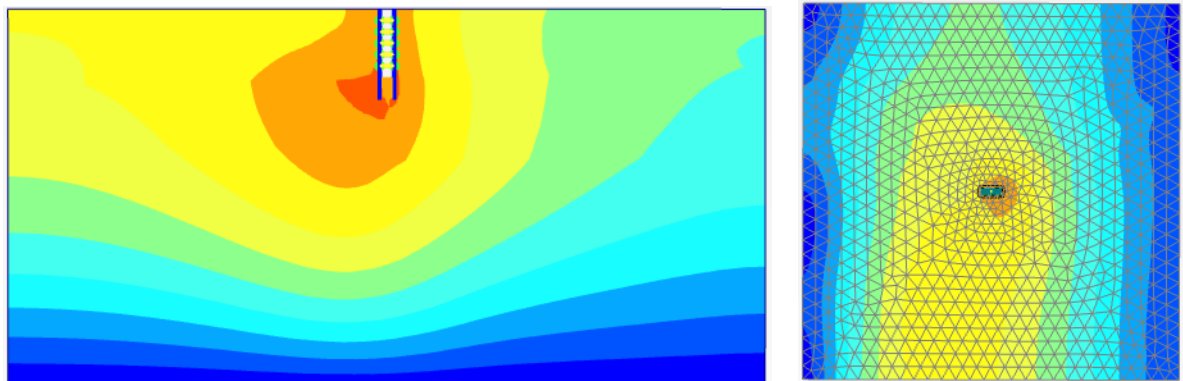


Figure.29. M-C model where total maximum displacement is 0,0299 m HEB 300 , model 100x200

2. HS-ss model variations results

The following table is a relation of the results given in the final calculation step the model.

Table.12 HS-ss results from model size variations where the area is change maintaining the same depth 100m

Last calculation step at -18 m	Measure	Units	100x160	100x200	100x260
	$ U $	[m]	8,264E-3	09,002E-3	0,024
	$ U_y $	[m]	1,534E-3	1,605E-3	4,724E-3
	M_{11}	[KN m/m]	210	257,8	148
	Q_{13}	[KN/m]	243	293,8	202,2

Where:

$|U|$ Total displacements; $|U_y|$ Horizontal displacements; M_{11} Bending moments; Q_{13} Shear force

It is clear the differences in the results from the 100x160 and the 100x 260 models in both cases. In the M-C the horizontal displacement 17% of difference and the HS-ss bending moment difference of 29% between the variations are a clear indicator that the dimension of the model affects in great extent the results.

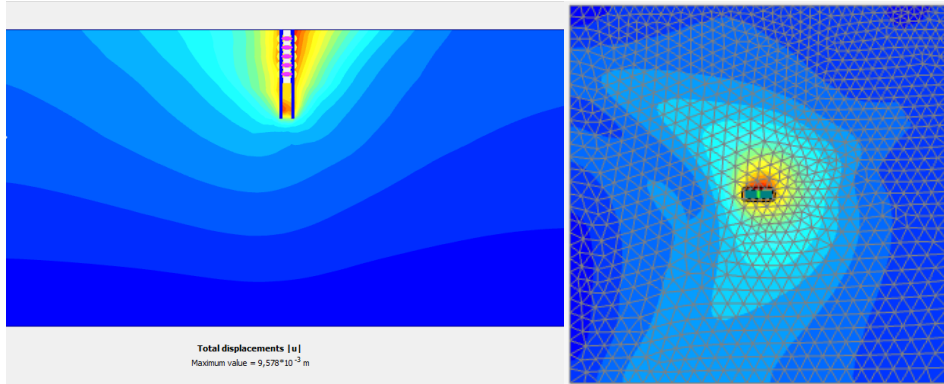


Figure.30. HS-ss model with HEB 300 , modell 100x200 with a maximum total displacement of 0,009578 m

It is worth to mention that using the same mesh size and the same distribution of the elements; in some cases and intervention in order to get the mesh of the model working, it was necessary to perform some local adjustment of the mesh in the walls of the shaft. This could have contributed to some extent on the differences of values for the variations especially in the HS-ss model and Mohr coulomb.

3. HS-ss models using struts HEB 300 and HEB 450 struts

The given design has used as a shoring system HEB profiles for the struts as well as for the wailing. The following is a relation of the results per excavation calculation steps with the HEB 300 and HEB 450 as a combine solution where the third and fourth level of the excavation are supported using a 450 profiles, all the rest of the levels are supported using a 300 HEB profile for struts and wailing.

The Struts used in the previous models have shown to be supporting an important amount of loads (see appendix. H and J), so a change on the struts and wailing used in this model is done to increment the support capacity. Under this kind of conditions in reality a different kind of shoring system will be use. One that will include support in the corners of the shaft and in some cases hydraulic jacks to provide pre-loading.

Table.13.HS-ss results from model size variations where the area is change maintaining the same depth of 100m

Measure	Units	Results after excavation levels					
		1	2	3	4	5	6
$ U $	[m]	0.0179	0.0189	0.0358	0.041	0.0367	0.010
$ U_y $	[m]	1.917E-3	7.053E-3	0.02136E-3	0.02501	0.01446	1.653E-3
M_{11}	[KN m/m]	23.70	23	42.33	89.86	178.6	193.5
Q_{13}	[KN/m]	28.05	64.63	71.58	137.4	196	246.7

Where:

$|U|$ Total displacements; $|U_y|$ Horizontal displacements; M_{11} Bending moments; Q_{13} Shear force

4. Verification of 3D model with struts HEB 300 using PLAXIS 2D AE model.

Based on the model parameters used in the 3D modelling used material parameters, underground pore pressure and support system a second analysis is done using Plaxis 2D the analysis is done using HS-ss models to analyze the behavior of the retaining system using a cross section representative of the 3D model variation (100x200). The only parameters that were changed is the amount of layers and the location of the layers as per boreholes M3 and M4 (the two boreholes used for this model in 2D, (See figure.26a.) all the rest of parameters part of the HS-ss model are used.

9.2. Model parameters

Geotechnical profile and shaft geometry and structural details:

Soil ID	γ_{unsat}	γ_{sat}	E'	φ	v	c'_{ref}	k_v	k_h
	[kN/m³]	[kN/m³]	[kN/m²]	[°]		[kPa]	[m/d]	[m/d]
A1	20	20.5	6000	28	0,3	1	0.864	0.864
A2	18.5	19	4500	34	0,3	0.1	0.000864	0.0432
B	20.5	21	8000	26	0,3	0.1	4.32	4.32
C	18	18.5	2700	24	0,3	0.1	0.000864	0.00864
D1	19.5	20	5900	27	0,3	0.1	0.864	0.864
D2	19.5	20	3800	30	0,3	0.1	0.0432	0.0432

Note: As a variant to results of the first study by M. Anthi, 2015 in the following 2D analysis as well as in the 3 D analysis all layers are analyzed by using HS-ss. This was done considering the material layers as well as to see in full extent the extent of the effects of the HS-ss model in the results.

<i>Struts</i>	
EA1	L
[kN]	[m]
3500000	6

<i>D - Wall</i>				
EA1	EI	d	w	v
[kN/m]	[kNm²/m]	[m]	[kN/m/m]	
2.40E+07	1.28E+06	0.80	4	0.15

Jet grouting slab						
γ_{unsat}	γ_{sat}	E'	v	kv	kh	R
[kN/m ³]	[kN/m ³]	[kPa]		[m/d]	[m/d]	
24	24	1.00E+06	0.2	8.64E-05	8.64E-05	1.00

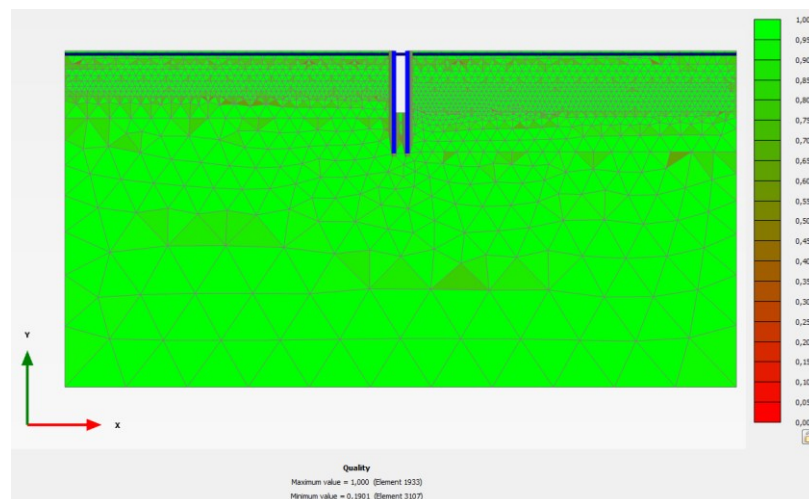


Figure 31. Asymmetrical model section Mesh quality where for layers A2, B, and C a fine mesh was used to further see the in more detail the behavior of this soil layers as layer B, the sand silty layer is the focus of this study.

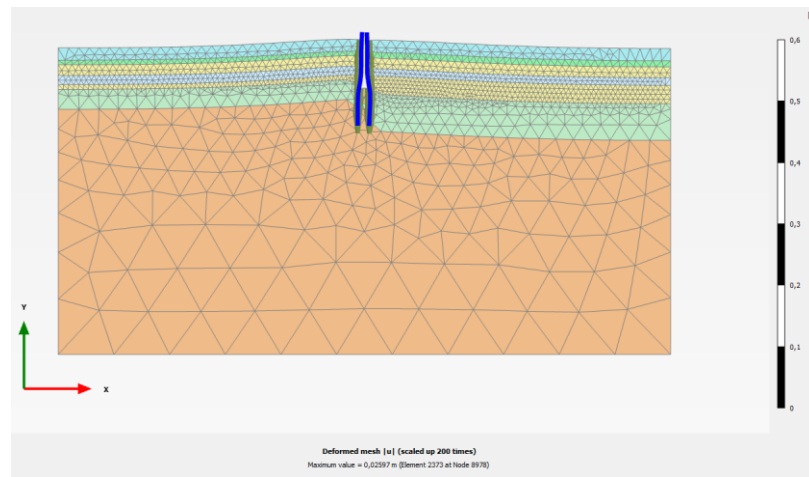


Figure 32. Asymmetrical model 100x200 section HS-ss model. Deformed mesh at the last excavation step.

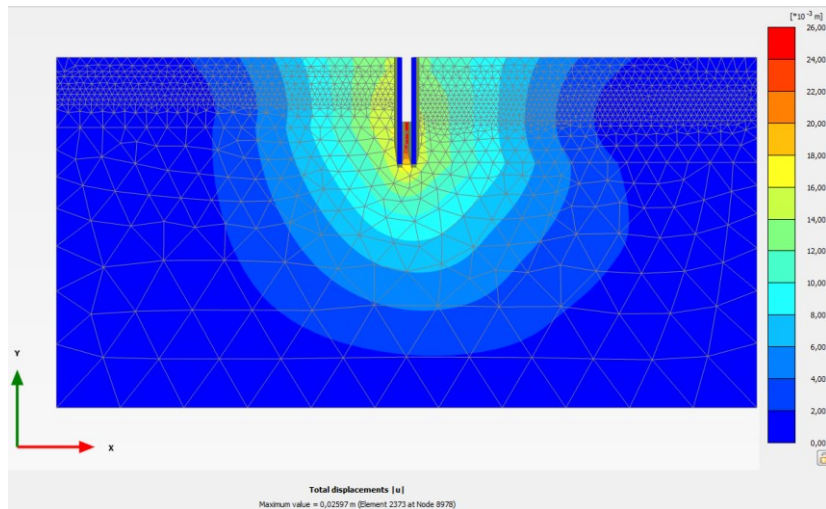


Figure.33. HS-ss model last excavation step with a maximum total displacement $|u|$) 0.01532 m

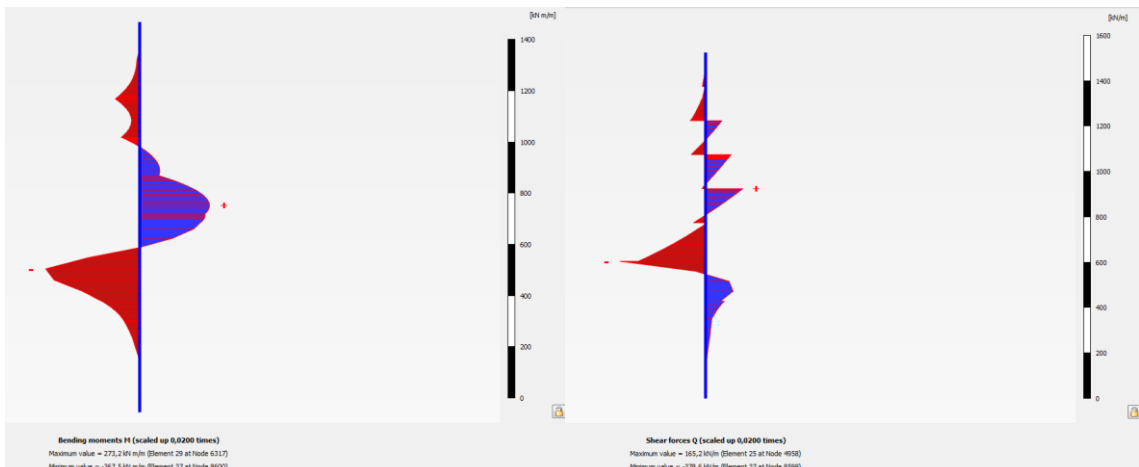


Figure.34. Maximum bending moment 273,2KNm/m and Shear forces 165KN/m at level -18 m.

The 2D model confirms the 3D model calculation by having a bending moment value of 273.2 KNm/m that is found in the range of the 3D model 257,8 KNm/m, as expected. (See table 12).

10. Layer B collapse

The geotechnical description of this layer (See table.1.) mentioned as a silty sand layer that is not well compacted and classified as a soft material. In this layer the intermediate or lower part of the free aquifer is found, has the highest hydraulic conductivity of all layers.

Silty sand can be described as the mixture of large sand grains and small grains of silt material. The proportion in which this two are present will determine the mechanical properties of layer B, both in the undrained and drained cases as the amount of silt particles could reduce the undrained shear strength of this layer. Silty sand stress-strain behavior is

dependent on the quantity of small particles within the soil matrix, therefore different grain arrangements within the same soil matrix provides a range of different stress-stain responses, (See figure.31.) (Ching S. Chang, and Zhen-Yu Yin, 2011).

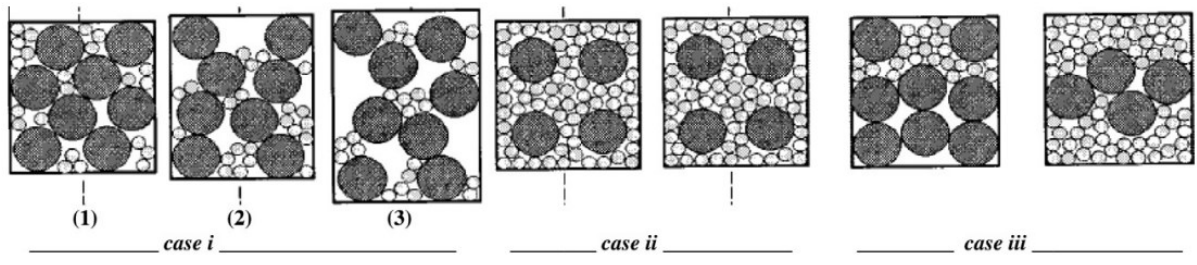


Figure.35. Inter granular soil matrix of large size grains (sand) and small grain size (silt). Thevanayagam et al., 2002.

The amount of silt particles has an influence on the quantity of sand particles that are interlocked, these results in a substantial change of void the void ratio. Ching S. Chang, and Zhen-Yu Yin, (2011).

From figure.31. It is possible to see how the sand grains can be isolated, and partially isolated, or floating in the small size grains, having a very limited bearing capacity in accordance with the slit content. This situation is represented in the collapse model, by the soft soil creep model where time should be considered for the consolidation to take place.

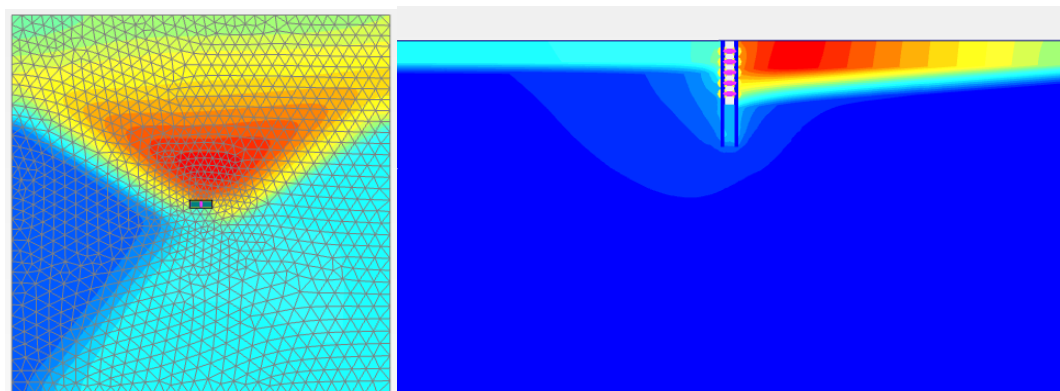


Figure.36. last step of the shaft excavation with a total maximum displacement value of 0,039m due to the collapse of the silty sand layer as we can see the part where the layer has more volume has been affected.

11. Sensitivity analysis

The sensitivity analysis is done by considering the action of side loads, 20KN/m² in the adjacent soils to the shaft during excavation where the struts used are HEB 450 in all levels.

Last step at -18 m	Measure	Units	Level -3	Level -6	Level -9	Level -12	Level -15	Level -18
	$ U $	[m]	0,05086	0,5104	0,05242	0,0531	0,05225	0,5210
	$ U_y $	[m]	2,151E-3	1,896E-3	6,973E-3	0,061E-3	5,706E-3	0,064E-3
	$ U_z $	[m]	-02665	-0,02584	-0,02482	-0,02380	-0,02276	-0,02182
	M_{11}	[KN/m]	22,11	21,54	93,28	111,6	150,3	177,6

Where:

$|U|$ Total displacements; $|U_y|$ Horizontal displacements; M_{11} Bending moments; Q_{13} Shear force

It is observed that the soils where this loads where apply at the end of the excavation had an impact of the existing soils due to the compression force that is like to cause the soft layer B to compress.(See appendix G and I).

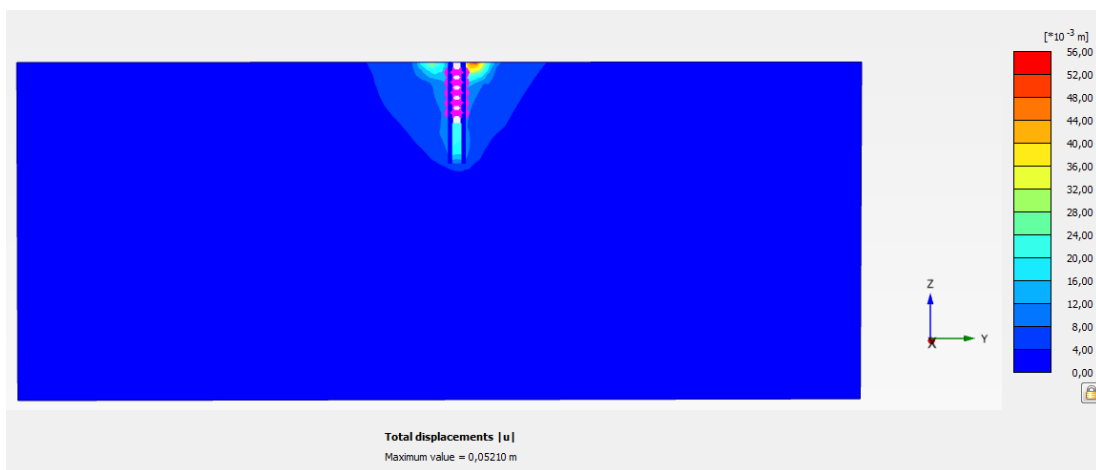


Figure.37. where the total displacements $|U| = 0,05210 \text{ m}$

12. Discussion.

The design of support systems requires the consideration of different factors that at the moment of performing a model one must take into consideration as the reasons for the possible behavior of the most critical materials and a further analysis of its behavior should be also part of the analysis in a second step to find the influence level of the critical materials.

Was the sand layer “B” important in the final behavior of the D-wall?

The soil layer B is composed by a soft layer of sand silty material that is said not to be compacted. After reviewing the results of the numerical analysis it is possible to see that that part of the wall movements takes place about the high where this layer is located. In the present model and due to the asymmetric geometry produced by the difference in levels by the existing soils, layer B, has on the right hand side of the shaft a larger contact area with the trasdos of the D-wall, and behind that same material is the clay layer C. Therefore, the silty sand layer is found between the D-wall and the clay layer. At the same time, the point where the layer B and the wall meet is the lowest point in layer B. Considering this situation an increment in the pore pressure at this point could explain the possible inflow of sand in the shaft, as it had happened during the construction of the shaft, as this is the point with more pore pressure. Silts particles are two small and can easily find their way through small openings or cracks, generating a sufficient change in the layer B soil matrix, changing the existing equilibrium conditions bringing the soils surrounding the wall to a collapse.

The geotechnical 3D model shows how these layers are changing significantly in the area where the shaft has been constructed, this area, acts as a convergence point not only for layers C and D. The trial shaft is relatively close to the existing buildings of the station as well as the Lucerne University building.

Any changes in the volume due to loss of the pore pressure of layer B, could become a risk for the existing constructions as this layer, can act under a quicksand effect allowing the removal of large quantities of fine material in a very short period of time, creating important subsidence in the near foundations including the rail tracks.

The construction of the panels that form the D-wall should consider the mentioned possibility when excavating, as the use of bentonite emulsions does not guarantee the support of the excavation trench, the sand content in the bentonite suspension used should not be more than 3%, continuous check on this particular is advanced.

D-Wall has to be done, having special attention to the joints between panels as well as the corners as in this places is usually where gaps could be created a large concentration of stress could be found in the corners of the shaft.

It is relevant to recall that the description of layer B, a slit sand layer, means a mixture of small size grains (Slit) and large grain size (sand). This same layer is included in the reservoir located in the upper part of the clay layer “C” the intermediate reservoir. Layer B has a high hydraulic conductivity, K value, both in the vertical and horizontal axis been the highest

when compared with the rest of the soil horizons part of the geotechnical profile. That means that sand is the predominant part in this soil layer as water flow occurs in both axes at the same rate. The quantity of silt within the soil matrix will determine the bearing capacity of layer B in the undrained case, as if the pores within the sand are filled by the small grains of silts the friction angle can be considerably reduced and so the bearing capacity of this layer, therefore any changes in the pore pressure in this layer could activate a collapse of the silty sand. For the analysis of the collapse model the friction angle will be used to find the critical friction angle of the silty sand layer B.

The area where the Lucerne Central station is located is above an antic encashment from where in different geological periods, large quantities of material were transported to the lowest point. Today's Lucerne Lake. This transit of weathered materials as well as sediments found in the west part of the city left behind thin layers and lenses of materials of different kinds. E.g. clays, silt, fine sands, making a very complex soil matrix. It is important therefore for the future development of the underground tracks at the central station, to perform a larger geotechnical survey, as the conditions under the station changes within meters. Usually we can offset the geotechnical properties of a borehole within 5 to 15 meters not having an important change in the final outcome; in the case of Lucerne Central station, this will represent the use of the wrong parameters. An extensive geo-geotechnical survey must be done to find a better description of the soils and their geotechnical properties that perhaps will yield the use of ground freezing techniques or injections of bacteria that could provide stability to those layers where the possibility of collapse due to excavation is imminent.

The sequence of the construction of the shaft could have an influence on the later behavior of the D-walls. Constructing the bottom slab after the construction of the diaphragm walls created an excess of pressure in the material found within the shaft that at the same time, has pushed the D-walls to the size creating a new set of tensions. This has assisted on the formation of openings or gaps in the D-wall. It is also important to mention that in such a case, layer B could be drastically affected as the silt within this sand layer after being pressed changes the disposition within the soil matrix, found in the sand and therefore its volume. It is also important to mention that the loading and unloading and reloading of the adjacent soils during the construction of the bottom slab, and during excavation, could drastically increase the failure of the shaft, not only affecting the walls of the shaft but the shaft as a unit.

The city of Lucerne has very strict rules regarding underground water contamination, being one of the main reasons for the design team of the trial shaft to go for such a deep bottom slab, where as in other cases, just by driving the D-walls into an impermeable layer will be sufficient.

The construction sequence is very important when working with soft soils. The use of jet grouting requires continuous monitoring of the build-up pressures within the surrounding soils and perhaps the injections should be done allowing the soil to deform by using several injection steps and therefore been able to see the impact on the walls as well as in the surrounding soils before fully completing the bottom slab as a single unit

13. Conclusions and recommendations

The design of shaft in soft soils requires an extensive amount of information, as in most cases this deposits have a complex layering or soil matrix that makes their analysis very singular due to its nature.

The assumption of values on the vicinity where the structure is planned to be constructed, are not sufficient and this trial shaft is a good example.

Due to the amount of error that could happen when changing material parameters, and in general model parameters, it is necessary to have ways of making some simple checks that allow us to continue with the calculations. Apart from this checks in the results it is also important when exporting model parameters to check that the parameters have been copied properly. Especially when running the same model using variations.

The displacement and the stress analysis show how the D-wall is affected by the different soil layers and their capacity as well as the exiting pore pressures. The plastic points clearly show the tendency of creating a failure plane in both sides of the shaft in different layers and in accordance with the friction angle of each layer, as in the case of the sand layers.

In the first steps of the excavation the displacements are larger than in the final state something that is not seem when using analytical solutions in a 2D analysis.

It is also seem that layer B, is very sensible. And can easily flow into the shaft e.g. via cracks in the wall the silty sand layer could rapidly fill the shaft excavation, especially in the side where the material from layer B is pressed the D-wall trasdos, by the layer clay C.(See appendix G).

As Plaxis is not calculating the safety factor of structural elements, it is necessary to stress the necessity of reviewing the bearing demands of structural members to properly select the correct material parameters as in the case of the HEB profiles 300.

14. Suggestions for future studies.

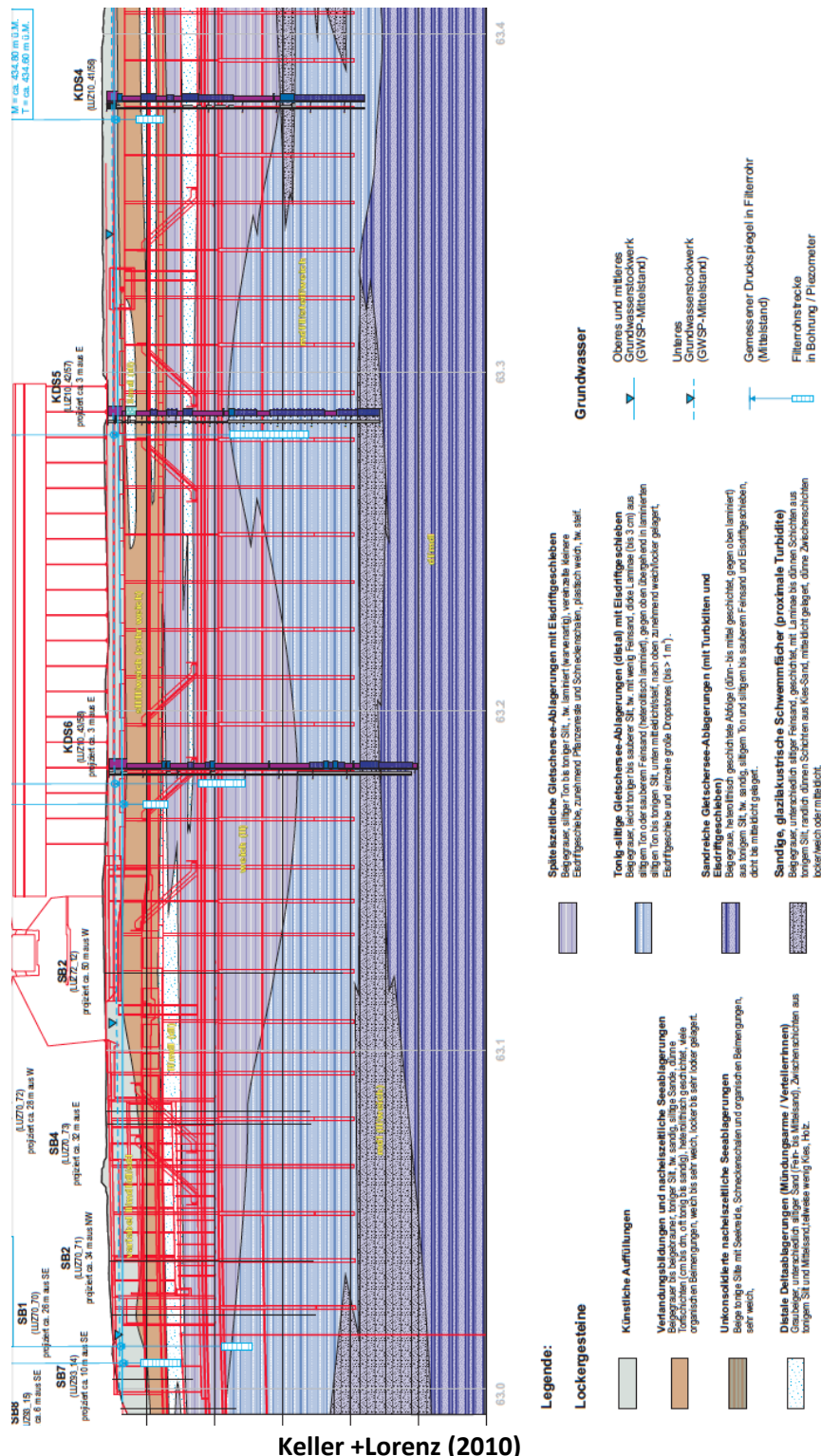
Now that the behavior of the soil most complex layers has been studied within this two studies, the present study and the previous by M. Antri, 2015, regarding the trial shaft of Lucerne Central station, some suggestion for the next study are made.

The analysis of the effects of excavations in the existing soils layers, by analyzing two main aspects.

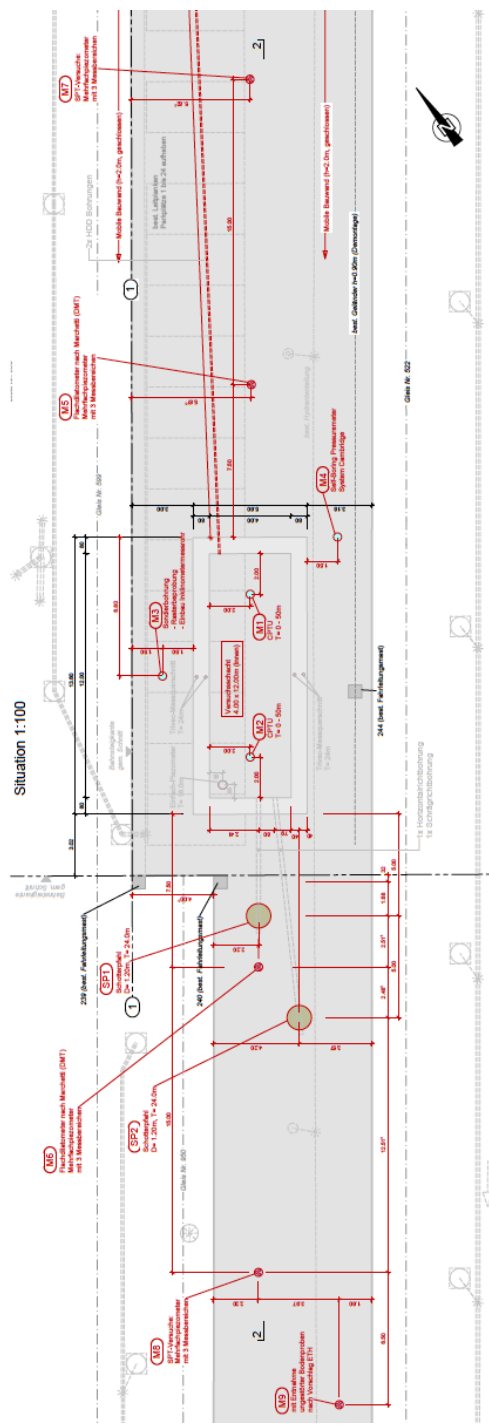
The first, aspect will be the influence of the construction of the bottom slab on the walls, adjacent soils, and soils to be excavated within the shaft, as it has been pointed in other studies that this was an important factor for the convergence experienced during the construction period.

The second aspect is the effects of the construction of the panels. This can be done using Plaxis2D and creating a cluster for the concrete wall using M-C model, as for the suspension material a soft soil model could be used to simulate the suspension material, that was used to retain the soils from caving while excavation was executed. The analysis could also be done by reproducing a 3D D-wall model, using cluster material under a M-C model for the shaft walls to see the effects of the deformation in the wall, and the corner effect where might be possible to see possible points where crack could appear in the wall.

Appendix A. Geological profile for the area where the future underground railway is planned

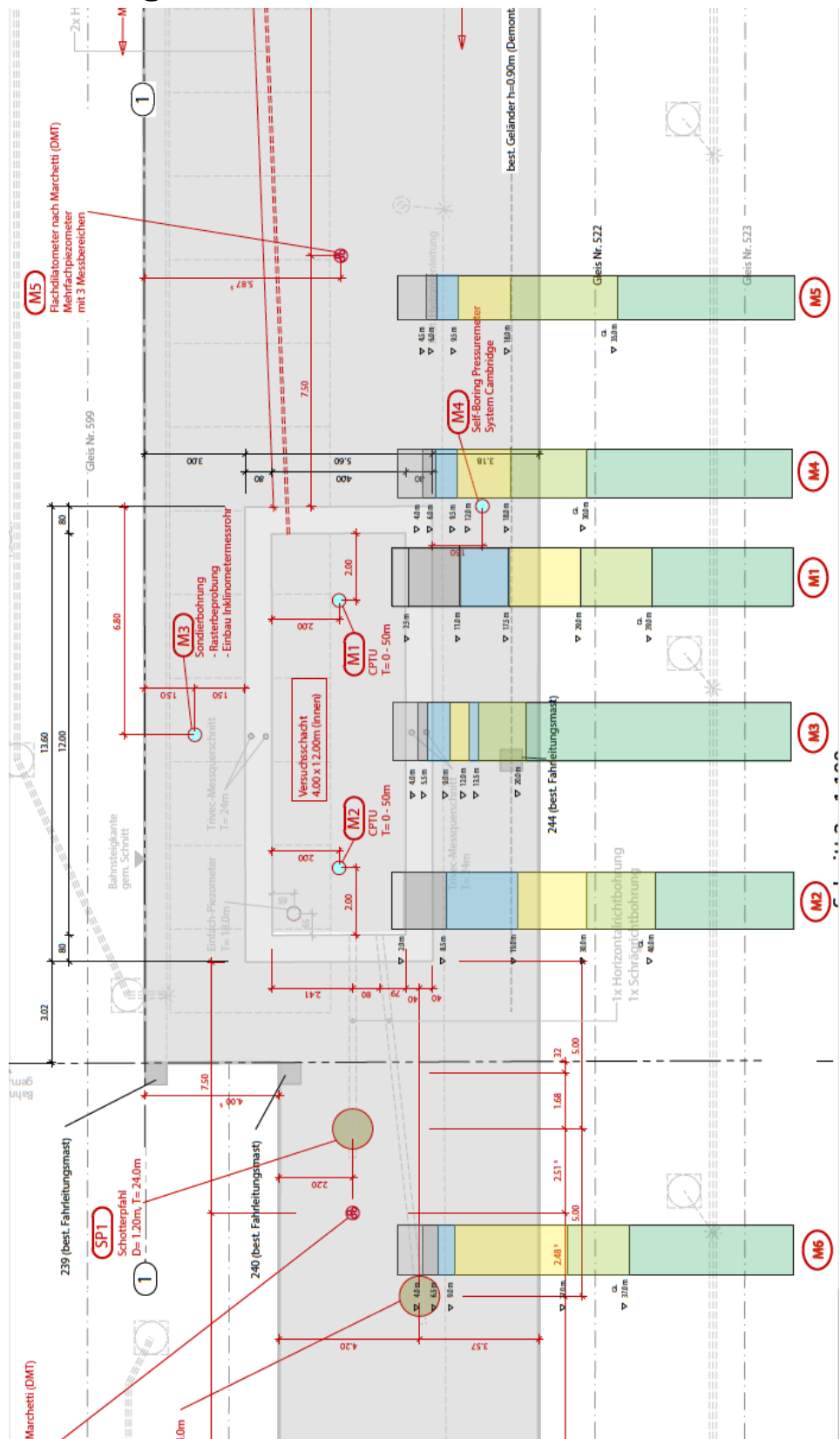


Appendix B . Floor plan of the trial shaft where the boreholes are used for the geotechnical profile and for the material properties (M9) are shown. B&H AG, 2012.



B&H AG, 2012.

Appendix C. Shaft with the allocation of the bore holes used for the 3D and 2D modelling.



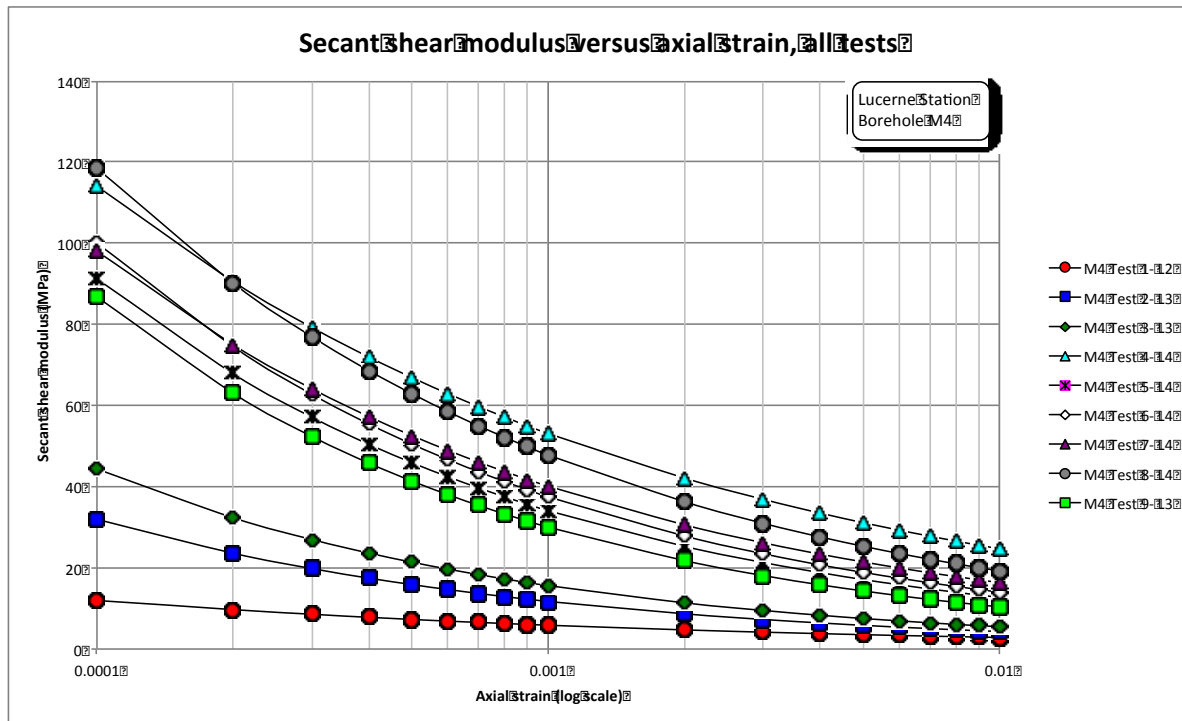
Appendix D. Odometer test results bore hole M9 and corresponding values for HS-ss.

Oedometerversuche IL (Lastgesteuert)											
M_E'	[kPa]	C				D1				D2	
		[MPa]									
Laststufe											
12.5	Load	0.7	1.2	1.0	1.2	1.4		1.3	1.7	1.2	1.9
25	Load	1.2	0.8	1.3	1.8	1.7	1.6	2.2	2.8	1.3	1.7
50	Load	1.8	2.8	2.3	3.2	2.4	4.5	3.5	4.5	2.1	2.4
100	Load	2.0	3.0	3.2	5.2	3.7	6.3	6.6	7.8	3.9	3.7
200	Load	2.2	2.8	3.3	7.9	5.6	11.3	10.4	11.3	7.1	5.6
400	Load	3.5	3.7	4.3	10.2	7.6	17.5	17.6	16.7	14.4	7.6
800	Load	8.3	8.8	8.9	18.3	11.8	31.4	34.0	27.2	13.9	11.8
1600	Load	15.0	15.4	16.0	27.7	19.0	43.0	47.2	33.6	15.3	19.0
200	Unload	93.0	88.9	70.2	121.2	95.2	117.6	133.3	160	85.1	95.2
100	Unload	24.1	25.6	19.4	44.4	19.0	46.5	52.6	50	17.2	19.0
50	Unload	8.7	8.7	7.4	16.4	5.7	17.9	26.3	21.3	6.4	5.7
100	Reload	20.0	19.2	17.2	34.5	10.2	31.3	52.6	35.7	11.0	10.2
200	Reload	19.8	19.8	16.3	33.9	12.1	37.7	44.4	42.6	14.3	12.1
400	Reload	19.5	22.6	17.9	40.4	17.5	37.0	54.1	57.1	32.0	17.5

Boden	$E_{50,\text{ref}}$ [kPa]	$E_{\text{oed},\text{ref}}$ [kPa]	$E_{\text{ur},\text{ref}}$ [kPa]
C	5630	2700	23657
D1	10973	5900	43714
D2	5478	3800	18617

Antri, 2015

Appendix E. Cambridge test results test results from where Go and $\gamma_{0.7}$ bore hole M4

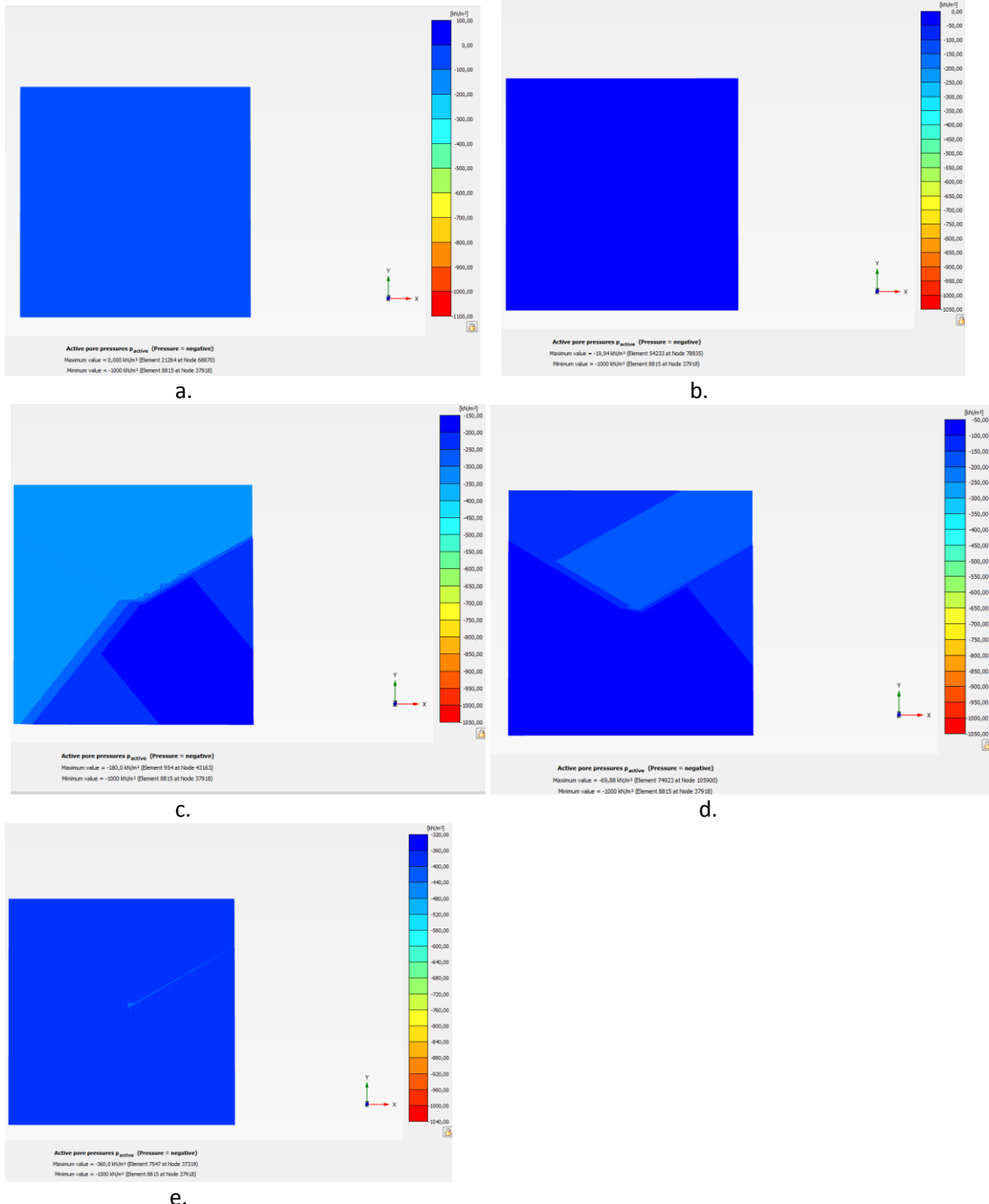


Auswertung

Schicht	G_0 MPa	gemittelt		$\gamma_{0.7}$	gemittelt
		-	-		
B	12	12.00	0.018%	0.018%	
C	32	38.50	0.020%	0.020%	
	45		0.020%		
	115		0.028%		
D1	92		0.023%	0.025%	
	100	101.00	0.024%		
	97		0.026%		
D2	120		0.025%	0.023%	
	87	103.50	0.021%		

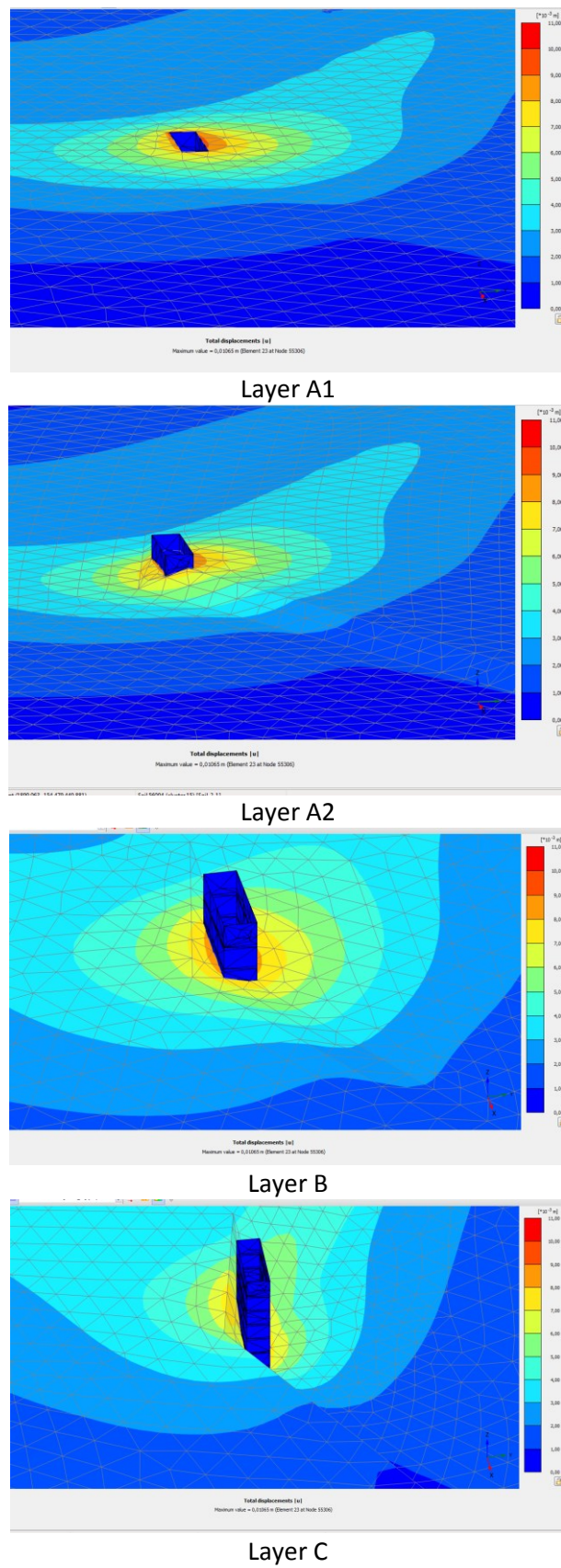
Antri, 2015

Appendix F. Pore pressures as per bore hole user define pressures.



The pore pressure as per material layer found in the model following the prescribe pressures for the artesian reservoir. a. A1 where the free reservoir is located ; b, A2 layer c; The not so compacted sand layer subject of analysis of this study d; Corresponding to the clay layer C, that serves as a division layer for the two existing reservoir and e. Sand layer where the artesian aquifer is located.

Appendix G. Relation of layers that are in contact with D-walls.



Appendix H. Bending moment 3D view and lateral displacement 300 HEB

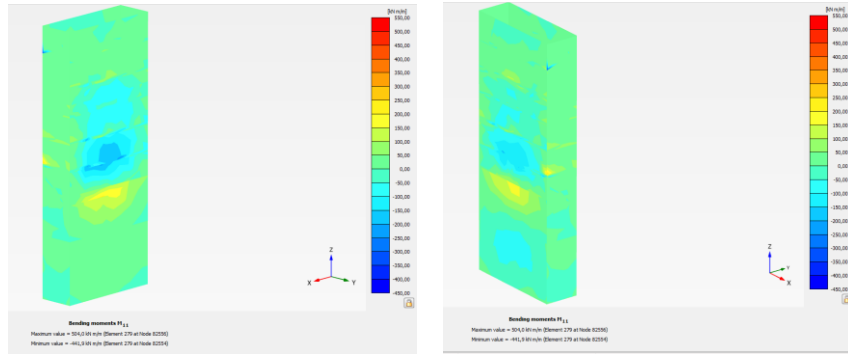


Figure.. Bending moments M_{11} where the same area that is shown in figure., for the displacements exhibits the larger bending moments.

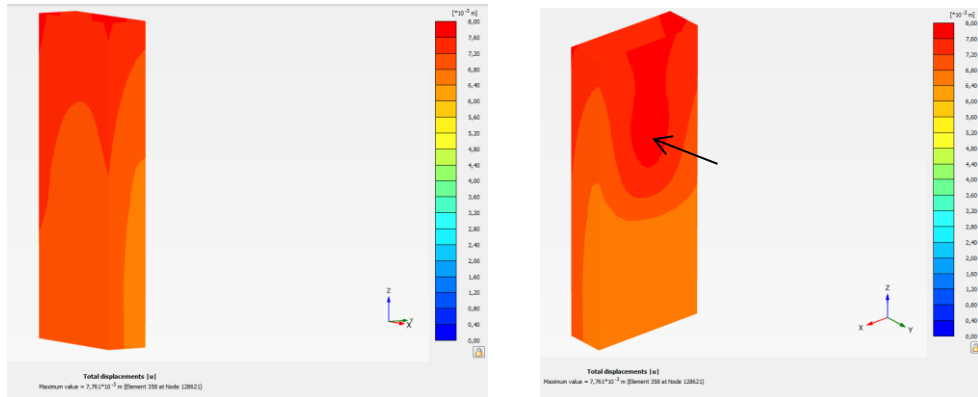


Figure.33. HS-ss model total displacement in D-wall in the right hand side of 7.76mm the arrow is showing the point where the maximum value for the displacement of the Dwall is located.

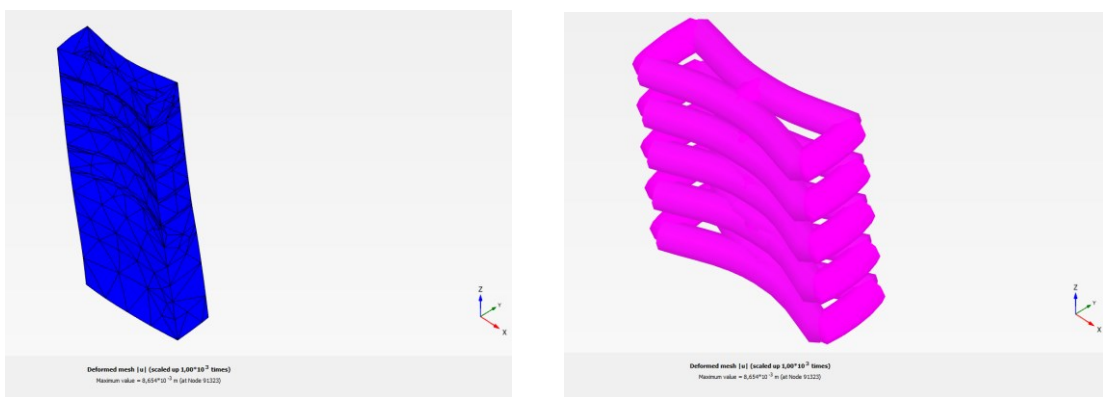
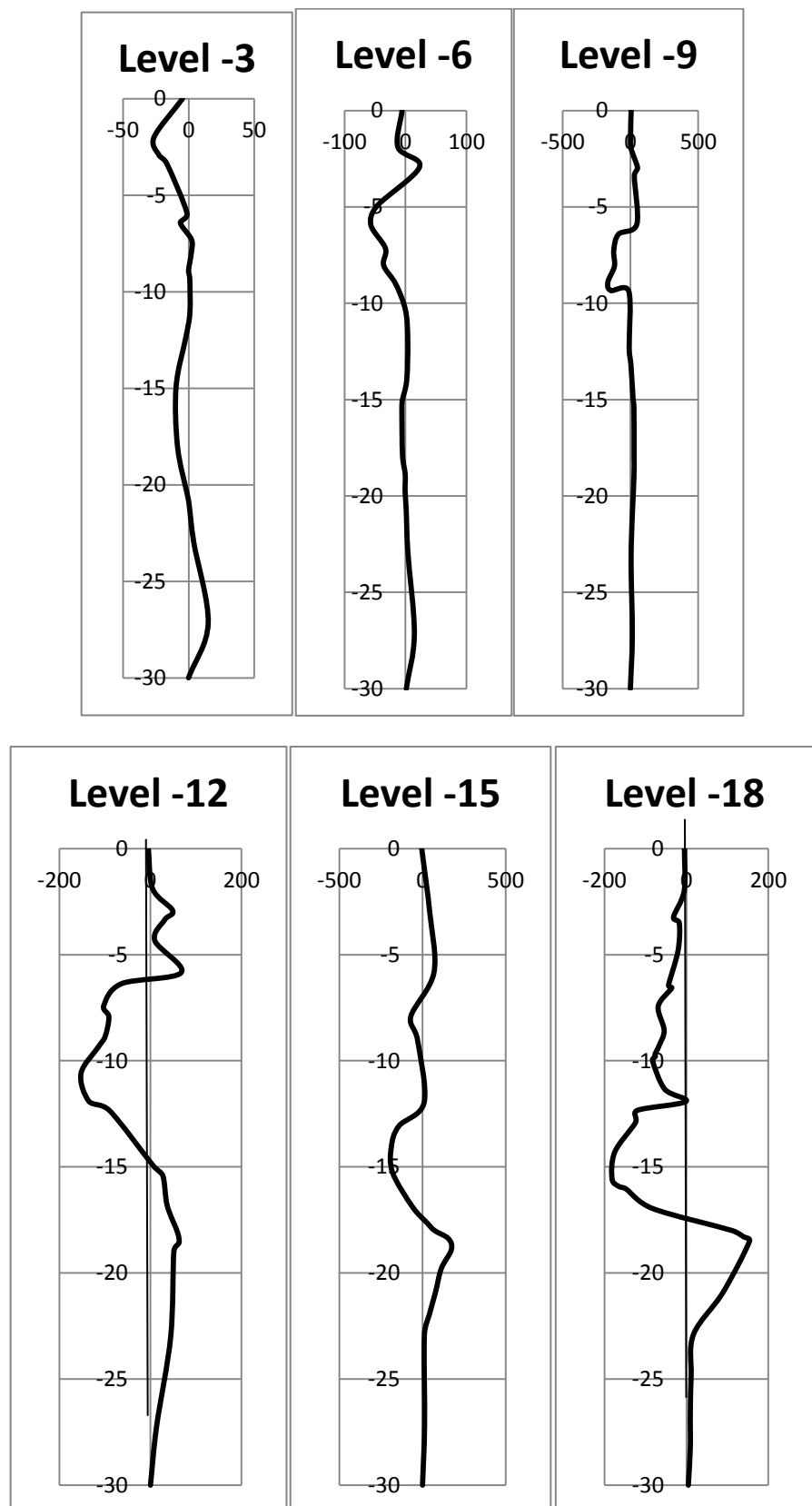
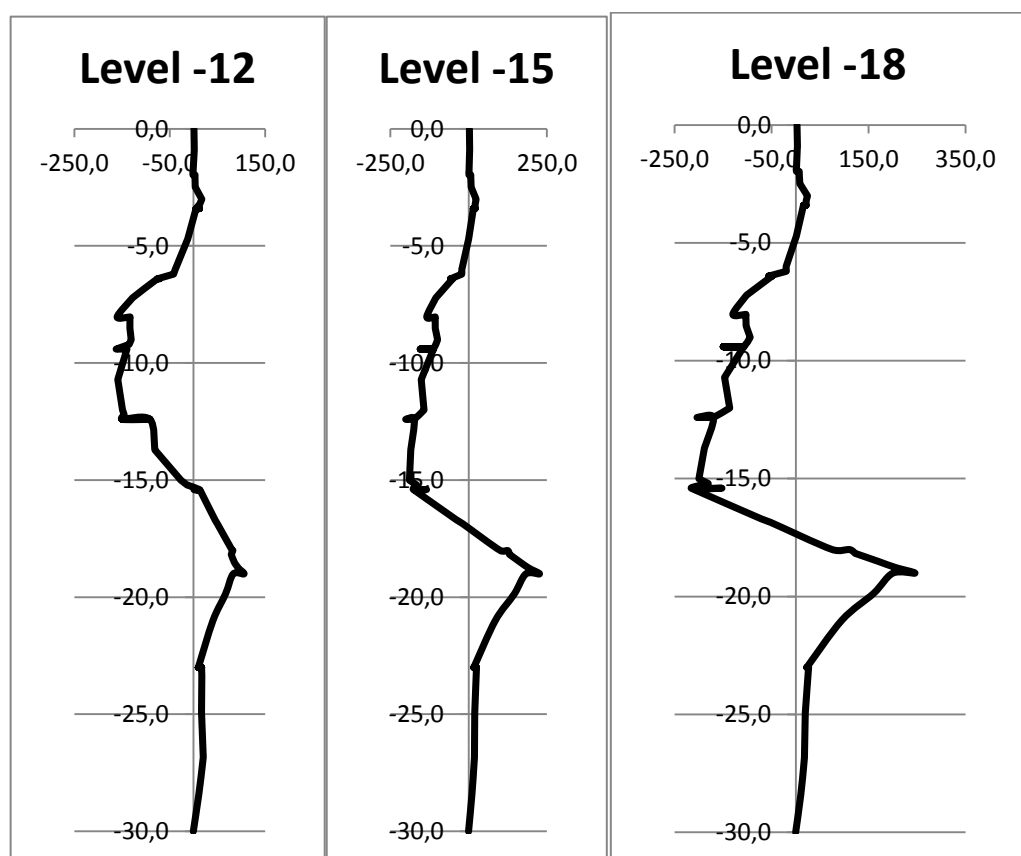
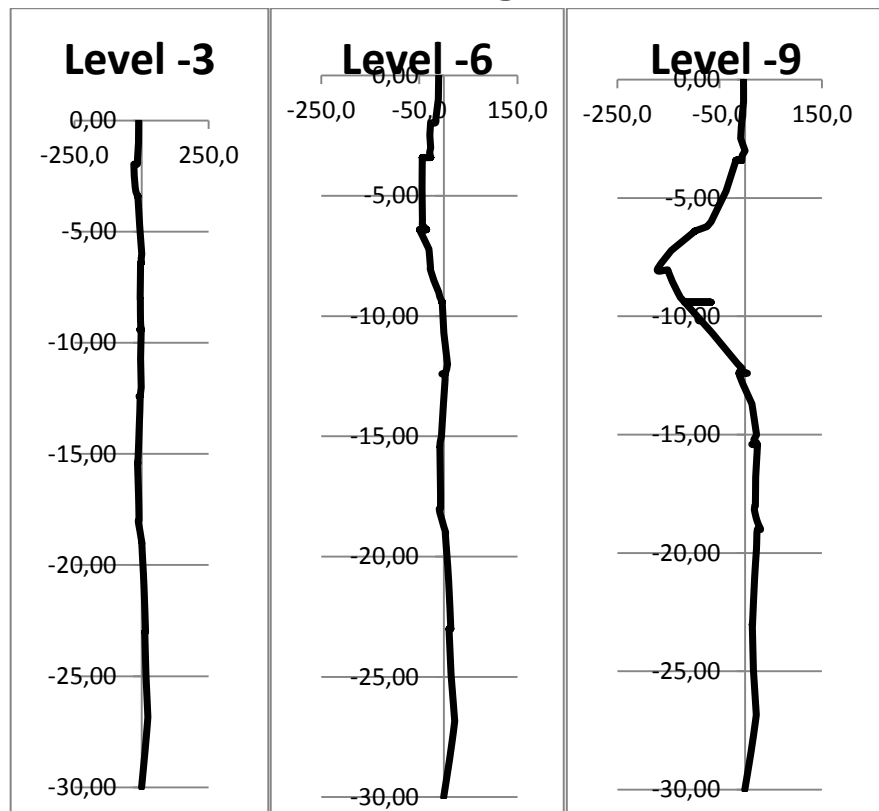


Figure.. shaft D-wall and Steel HEB profile shoring frames after last step of the excavation

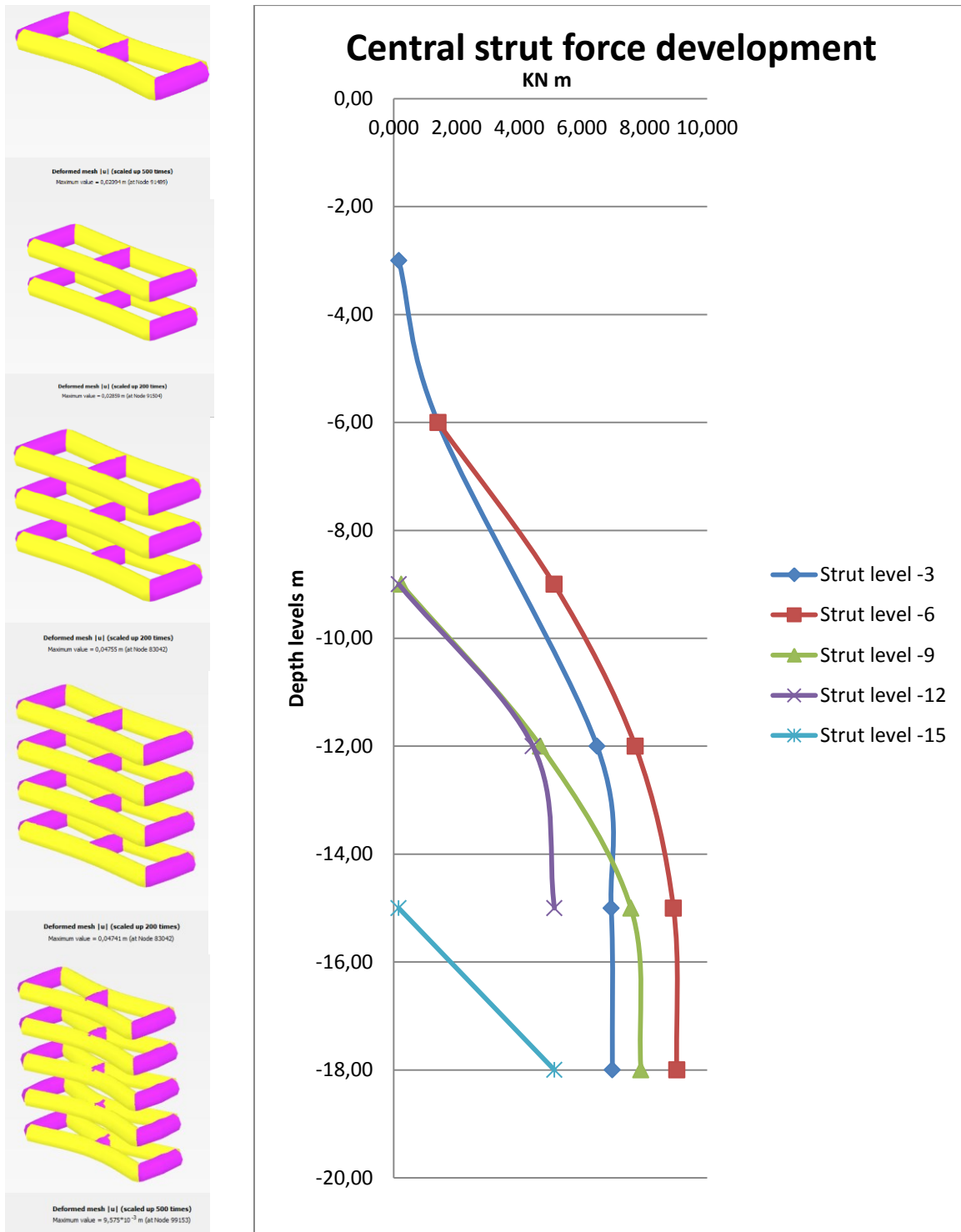
**Appendix I. D-wall ending moments HS-ss model HEB 300 and 450
100x200**



Appendix J. 3 D model. D-wall bending moments HS-ss HEB 300



Appendix K. Struts forces by construction steps HEB 300



Literature.

1. Maria Anthi,(2015). Der tiefbahnhof Luzern Eine Fallsstudie des Versuchsschachts mit plaxis 2D Luleå, Sweden.
2. TP Labhart, (1987). Geology of Switzerland Hallwag Publishers, 4th edition,
2. Ernst & Sohn, (2003). Geotechnical engineering handbook Volume 3: Elements and Structures pg. 274-403 Darmstadt, Germany.
3. Luc Delattre, (2001). A century of design methods for retaining walls – The French point of view.France Pg. 34- 49
- 3.3D Plaxis, (2012). Tutorial manual
4. Plaxis, (2015). Material manual
5. G.Zhang, Robertson, (2004). Estimating Liquefaction induced Lateral Displacements Using the Standard penetration Test or Cone Penetration Test, 10.1061(ASCE), Journal of geotechnical and geoenvironmental engineering ASCE pg.861-869
6. C.Rbalotti, (2015). Instrumented test shaft in soft ground FMGM Australian Centre for Geomechanics, Perth Sydney, Australia
7. Carlo Rabaiotti et al, (2014). Pre-Stressing of soil and structures due to jet grouting, ICE London, UK
8. Ching S. Chang, Zhen –Yu Yin, (2011) Micromechanical modeling for behavior of silty sand with influence of fine content. Amherst, Ma, USA.